

FLOW ANALYSIS OF MULTIPURPOSE LOW CAPACITY TURBINES USING CFD

A DISSERTATION

*Submitted in partial fulfillment of the
requirements for the award of the degree*

of

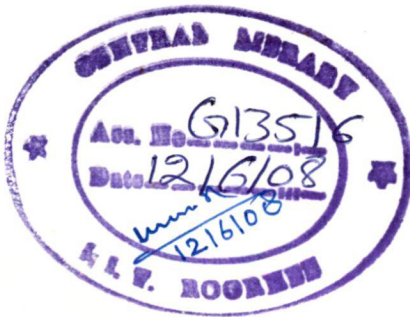
MASTER OF TECHNOLOGY

in

ALTERNATE HYDRO ENERGY SYSTEMS

By

KHALID RAZI



ALTERNATE HYDRO ENERGY CENTER
INDIAN INSTITUTE OF TECHNOLOGY ROORKEE
ROORKEE - 247 667 (INDIA)

JUNE, 2007

CANDIDATE'S DECLARATION

I hereby declare that the work presented in the dissertation entitled “**Flow Analysis of Multipurpose Low Capacity Turbines Using CFD**” submitted in partial fulfillment of the requirements for the award of degree of **Master of Technology** in **Alternate Hydro Energy Systems** in the Department of Alternate Hydro Energy Centre, Indian Institute of Technology Roorkee, is an authentic record of my own work carried out from July 2006 to June 2007 under the guidance and supervision of **Dr. R.P. Saini**, Associate Professor, Alternate Hydro Energy Centre & **Shri Arun Kumar**, Head of the Department, Alternate Hydro Energy Centre.

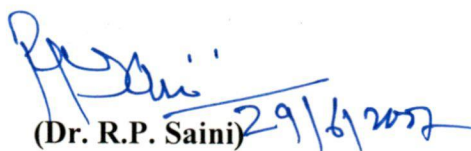
The matter embodied in the dissertation has not been submitted by me for the award of any other degree.

Date: June²⁹, 2007

Place: Roorkee


(Khalid Razi)

This is to certify that the above statement made by the candidate is correct to the best of our knowledge.


(Dr. R.P. Saini) 29/6/2007

Associate Professor

Alternate Hydro Energy Center
Indian Institute of Technology,
Roorkee


(Arun Kumar)

Head of the Department

Alternate Hydro Energy Center
Indian Institute of Technology,
Roorkee

ABSTRACT

In hilly region micro hydro up to 100 kW have momentous role in utilization of mechanical power and electricity generation. The capacity of micro hydro power plant up to 5.0 kW is considered under development of water mill program by Ministry of New and Renewable Energy (MNRE), Govt. of India. The popularity of the turbines under micro hydro lies in the fact that they are less costly and can be fabricated locally. There are various types of turbines that can be used in micro hydro. Cross-Flow turbine has been considered techno-economically viable for such sites.

Cross flow type runner can be fabricated locally, which results in the poor efficiency. The vanes can be made even from the pipes cut along the length. Also this kind of runner is suitable for low discharge and high head conditions which is a common case in the hills. A cross flow type runner has a drum shape consisting of two parallel discs connected together by a series of curved vanes or blades. The water from the nozzles strikes the vanes and convert $2/3^{\text{rd}}$ part of the potential into the mechanical power. The water that comes out from this blade strikes the diametrically opposite vane and the remaining conversion of $1/3^{\text{rd}}$ part takes place.

The problem with the fabrication of cross flow turbine runner at the local level is that its efficiency decreases due to lack of proper design and fabrication. The low efficiency is the basic inspiration to improve the existing design of cross flow runner. This study presents the flow analysis of a cross flow runner using Computational Fluid Dynamics (CFD). The runner was modeled on the CAD software Pro-Engineer and was imported to GAMBIT where it was meshed. The meshed model was imported to the CFD software FLUENT. The flow analysis was carried out on FLUENT.

The cross flow turbine has a through shaft for the rotation of the runner. It is observed that the size of this shaft offers resistance to the flow in between two stages. This study intends to study the flow pattern obtained by varying the size of the shaft. The results of this analysis can be used to study the flow pattern in a cross flow runner for suggesting improvements.

ACKNOWLEDGEMENT

I would like to express my deep sense of gratitude and indebtedness to my guides **Dr. R.P. Saini**, Associate Professor, Alternate Hydro Energy Centre, and **Shri Arun Kumar**, Head of the Department, Alternate Hydro Energy Centre, Indian Institute of Technology Roorkee, India for guiding me to undertake this dissertation as well as providing me all the necessary guidance and support throughout this dissertation work. They have displayed unique tolerance and understanding at every step of progress, without which this dissertation work would not have been in the present shape.

I would also like to thank **Shri Arun Kumar**, Head of the department, **Dr. R.P Saini**, Post Graduate Course Coordinator of Alternate Hydro Energy Center, IIT Roorkee for providing the necessary facilities to carry out the thesis work specially the procurement of the CFD software in the Center itself.

I would like to thank the staff of Alternate Hydro Energy Center for their constant support at all times.

I would also like to thank all my friends, for their help and encouragement at the hour of need. Finally I would like to mention my parents who are with me all the times to assist me with their caring and affection right from my childhood.

Date: June , 2007

Place: Roorkee

(Khalid Razi)

CONTENTS

<i>Candidate's Declaration</i>	<i>i</i>
<i>Abstract</i>	<i>ii</i>
<i>Acknowledgements</i>	<i>iii</i>
<i>Contents</i>	<i>iv</i>
<i>List of Tables</i>	<i>vii</i>
<i>List of Figures</i>	<i>viii</i>
<i>Nomenclature</i>	<i>xi</i>
CHAPTER 1 INTRODUCTION AND LITERATURE REVIEW	1
1.1 Introduction	1
1.2 Importance of Micro Hydro	3
1.3 Micro Hydro in Himalayan Region	4
1.4 Turbines suitable for Micro Hydro Range	5
1.4.1 Impulse Turbines	5
1.4.1.1 Pelton Wheel	5
1.4.1.2 Turgo Impulse Turbine	6
1.4.1.3 Cross Flow Turbine	7
1.4.2 Reaction Turbines	9
1.4.2.1 Francis Turbine	9
1.4.2.2 Propeller Turbine	9
1.5 Concept of CFD	10
1.5.1 Applications of CFD	10
1.5.2 Strategies of CFD	10
1.5.3 Discretization using Finite Volume Method	11
1.5.4 Assembly of discrete system and Boundary Conditions	12
1.5.5 Direct and Iterative Solvers	13
1.5.6 Explicit and Implicit Schemes	15

1.6	Objective of Present Study	16
1.7	Literature Review	17
CHAPTER 2	DESIGN OF CROSS FLOW TURBINE	22
	RUNNER	
2.1	General	22
2.2	Sizing of the Turbine	22
	2.2.1 Site Data	22
	2.2.2 Steps of Design	22
	2.2.2.1 Blade Geometry	22
	2.2.2.2 Design for the given Data	24
CHAPTER 3	MODELLING, MESHING AND THE SOLVER	27
3.1	General	27
3.2	Solid Modeling	28
	3.2.1 Pro/ENGINEER	28
	3.2.1.1 Properties of Pro/E	29
	3.2.2 Blade Profile	30
3.3	Modeling of Cross Flow Runner	31
3.4	Meshing	34
	3.4.1 Connectivity based classification	35
	3.4.1.1 Structured Meshes	35
	3.4.1.2 Unstructured Meshes	35
	3.4.1.3 Hybrid Meshes	35
	3.4.2 Element Based Classification	35
	3.4.3 Meshing of Cross Flow Runner	37
	3.4.3.1 GAMBIT	37
3.5	FLUENT- The Solver	41
	3.5.1 General	41
	3.5.2 Program Capability	41
	3.5.3 Basic Steps of CFD Analysis using	43
	FLUENT	

3.5.4	FLUENT in the Present Study	44
3.5.4.1	Solver	44
3.5.4.2	Viscous Model	45
3.5.4.3	Material	46
3.5.4.4	Units	46
3.5.4.5	Operating Conditions	46
3.5.4.6	Boundary Conditions	46
3.5.4.7	Initializing the solution	47
3.5.4.8	Iterations	47
CHAPTER 4	ANALYSIS	48
4.1	General	48
4.2	Analysis	49
4.2.1	Shaft with diameter of 50.8 mm	49
4.2.2	Shaft with diameter of 38.1 mm	53
4.2.3	Shaft with diameter of 25.4 mm	56
4.2.4	Shaft with diameter of 12.7 mm	59
4.2.5	Runner with no shaft	62
4.2.6	Full Runner with shaft diameter of 50.8 mm	65
4.3	Comparison between different models	68
CHAPTER 5	CONCLUSIONS AND RECOMMENDATIONS	69
5.1	Conclusions	69
5.2	Recommendations for Future work	71
	References	72

LIST OF TABLES

<i>Table No.</i>	<i>Caption of Table</i>	<i>Page No.</i>
1.1	Small Hydro Installed Capacity Worldwide	2
1.2	International Definition of Small Hydro	3
1.3	Classification of Small Hydro	3
1.4	Classification of Conventional Hydro Turbines based on Head	5

LIST OF FIGURES

<i>Figure No.</i>	<i>Caption of Figure</i>	<i>Page No.</i>
1.1	A Pelton Wheel	6
1.2	Water Impingement on Turgo Runner	6
1.3	Cross Flow Runner	7
1.4	The runner of Francis Turbine	7
1.5	Rectangular Cell showing faces and cell center	12
2.1	Geometry of Blades of Cross Flow Turbine	23
3.1	The blade geometry as drawn on Pro-Engineer	30
3.2	General view of Extruded blade	31
3.3	Model of the runner with shaft diameter of 12.7 mm	33
3.4	Model of the runner with shaft diameter of 25.4 mm	33
3.5	Model of the runner with shaft diameter of 38.1 mm	33
3.6	Model of the runner with shaft diameter of 50.8 mm	33
3.7	Model of the runner with no shaft	34
3.8	Model of full runner with shaft diameter 5.8 mm	34
3.9	2D Quadrilateral and Triangular Mesh elements	37
3.10	3D Hexahedra, Tetrahedral and Triangular prism mesh elements	37
3.11	Meshed Model with shaft diameter of 12.7 mm	39
3.12	Meshed Model with shaft diameter of 25.4 mm	39
3.13	Meshed Model with shaft diameter of 38.1 mm	39
3.14	Meshed Model with shaft diameter of 50.8 mm	39
3.15	Meshed Model with no shaft	40
3.16	Meshed Model of Full Runner	40
4.1	The Velocity Contours of runner with shaft diameter of 50.8 mm	50
4.2	The plot of Velocity Magnitude with respect to the position	50

4.3	The Contours of Static Pressure for the runner with diameter of 50.8 mm	52
4.4	The Plot of Static Pressure with respect to the position	52
4.5	The Velocity Contours of runner with shaft diameter of 38.1 mm	54
4.6	The plot of Velocity Magnitude with respect to the position	54
4.7	The Pressure Contours of runner with shaft diameter of 38.1 mm	55
4.8	The Plot of Static Pressure with respect to the position	55
4.9	The Velocity Contours of runner with shaft diameter of 25.4 mm	57
4.10	The plot of Velocity Magnitude with respect to the position	57
4.11	Contours of Static Pressure for runner with shaft diameter of 25.4 mm	58
4.12	The Plot of Static Pressure with respect to the position	58
4.13	The Velocity Contours of runner with shaft diameter of 12.7 mm	60
4.14	The plot of Velocity Magnitude with respect to the position	60
4.15	Contours of Static Pressure for runner with shaft diameter of 12.7 mm	61
4.16	The Plot of Static Pressure with respect to the position	61
4.17	The Contours of Velocity with runner with no shaft	63
4.18	The Velocity Plot of runner with no shaft	63
4.19	Contours of pressure for the runner with no shaft	64
4.20	The Plot of Static Pressure with respect to the position	64

4.21	Unsteady Formulation of shaft with diameter 50.8	66
4.22	The plot of velocity with respect to the position	66
4.23	Contours of pressure for the unsteady formulation	67
4.24	The plot of pressure with respect to the position	67

NOMENCLATURE

kW	=	Kilowatt
MW	=	Megawatt
R_1	=	Outer Radius of the Runner
R_2	=	Inner Radius of the Runner
β_1	=	Outer Blade Angle
β_2	=	Inner Blade Angle
r_b	=	Curvature Radius of the Blade
r_p	=	Pitch Circle Radius
δ	=	Segment Angle of the Blade
ϕ	=	Angle in radius between two points on the Spiral and the origin of the Spiral
e	=	Natural Logarithm
K	=	Cotangent of the angle between the tangent to the logarithmically Spiral
Q	=	Discharge
b	=	Inlet Width
ϕ°	=	Admission Arc Angle
H	=	Net Head
α	=	Angle of Absolute Velocity
L	=	Admission Arc Length
P	=	Pressure
V	=	Velocity
u_i	=	Velocity at the i^{th} Grid Point
Δx	=	Distance between two consecutive Grid Points.
\hat{n}	=	Outward Normal to the Surface
C	=	Courant Number
\vec{V}	=	Net Velocity Vector

CHAPTER 1

INTRODUCTION AND LITERATURE REVIEW

1.1 INTRODUCTION

Energy plays a significant role in the economical and technological development of the modern society. The conventional sources of energy are exhaustible. The starting point energy crisis is the oil crisis. As the awareness came in early seventies also came the search for the alternatives. Also it was required that the alternatives should be such that there should not be the major changes required in the system. Renewable energy emerged as the best option. The major renewable are hydro, solar, wind and biomass. The beauty of these renewable energy systems is that they are non-exhaustible.

Hydropower is the most promising among all the renewable energy sources. It is a clean source of power produced when the water turns a hydraulic turbine. It provides the electricity essential for the economic and social development of the society. The most important fact to be noticed is that the maximum potential of the hydropower is yet to be harnessed in many countries. Though hydropower development started with small units in the beginning, attention was diverted to harnessing medium and small hydro because of their comparative economics. India has a large potential in the medium and large projects. The inherent drawbacks associated with large hydro are the large gestation period, large area along with the vegetation has to be submerged which results in relocation as recently happened in the Tehri Hydro Power Plant. Political and environmental implications have compelled the planners to think for some other alternative of these large hydro resulting in the emergence of small hydro.

Of all the non-conventional renewable energy sources, small hydro represents the 'highest density' resource and stands in the first place in generation of electricity from such sources throughout the world. Emanating from the environmental and depleting conventional sources consciousness, there is an increased thrust on small hydro development in India. Government of India has stimulated considerable enthusiasm in providing speedy development of small hydro. SHP acts as the small centers for power

generation even in the remote areas where the basic needs of discharge and head are fulfilled thus emerging as an answer to the search for alternative energy source.

India has a history of 100 years of Small Hydro since its first installation of 130 kW at Darjeeling in the year 1897. India has one of the world's largest Irrigation Canal networks with thousands of Dams and Barrages. It has monsoon fed, double monsoon fed as well as snow fed rivers and streams with perennial flows. An identified potential of more than 10,000 MW [2] of small hydro exists in India, though overall potential of 15,000 MW [2] is anticipated. The installed capacity as on 31.3.2005 is 1705.23 MW with an additional 479.29 MW [2] under construction. World installed capacity of small hydro today is around 50,000 MW against an estimated Potential of 180,000 MW. A general scenario of Small Hydro installed capacity worldwide is as under:

Table 1.1: Small Hydro Installed Capacity Worldwide [2]

COUNTRY	INSTALLED CAPACITY(MW)
India	1,700
Japan	3,900
China	15,000
Rest of Asia	400
Europe	9,000
Rest of the world	20,000
Total	50,000

There is a general tendency all over the world to define Small Hydro by Power Output. Different Countries have different norms keeping the upper limit ranging from 5 to 50 MW as shown in Table 1.2. In India, small hydro schemes are further classified by the central Electricity Authority (CEA) as shown in Table 1.3.

Table 1.2: International Definition of Small Hydro [2]

COUNTRY	DEFINITION (MW)
UK (NFFO)	< 5
UNIDO	< 10
Sweden	<15
Colombia	<20
Australia	<20
India	<25
China	<25
United States	<30
Brazil	<30
Philippines	<50
New Zealand	<50

Table 1.3: Classification of Small Hydro Schemes [3]

TYPE	STATION CAPACITY	UNIT CAPACITY
Micro Hydro	Up to 100 kW	Up to 100 kW
Mini Hydro	101 kW to 2000 kW	101 kW to 1000 kW
Small Hydro	2001 kW to 25000 kW	1001 kW to 5000 kW

1.2 IMPORTANCE OF MICRO HYDRO

Micro hydro is the subset of small hydro with capacity up to 15 kW [2]. Micro hydro is an important player in the remote, hilly and unelectrified areas of India where there is a substantial potential that can be tapped. Thus, micro hydro is an answer to the rural electrification in the remote areas where potential exists. The power potential of 18790 MW is available in the micro hydro range and it is ready to be harnessed. The current concern on the global environment has imposed a new constraint on the production of electricity. The emphasis is put on the development of environmental friendly form of energy to promote the sustainable social development. It is in these

circumstances that the micro hydro power is drawing more attention. A rural population is scattered and unaware of the technological developments. For such areas, the isolated micro-hydro power plants are the least cost options. This is mainly because the other options for supply such as grid extension, diesel power, etc are more expensive and difficult to install or operate in the long run.

Since small water streams are usually available in the most of the region, micro-hydro power plants can easily meet the needs of small village or cluster of settlements. These needs may be in the form of electricity or motive power to be used for agro processing, wood working and for the other small scale industries.

Apart from numerous advantages that the micro hydro schemes offer there is some drawbacks associated with it also. Two of the most common drawbacks of micro hydro installations are lack of economical viability and inappropriate capacity. In the former case the installation either falls in disrepair or will sooner or later stop being operational or it drains resources which could be put to much better use. In the latter case, the installations will either not be able to meet the demand or it will not be used to its full potential, resulting in the waste of capital.

1.3 MICRO HYDRO IN HIMALAYAN REGION

In India, the micro hydro potential mainly exists in Himalayan and sub-Himalayan as there are plenty of small water resources in this region. From last many centuries the water mills are being used in almost all the continents, which come under the micro hydro category. People at that time found it as an important way to harness the enormous amount of energy that nature has stored within itself.

The potential in micro hydro range may be estimated based on the number of water mill sites. With over 200,000 water mill sites existing in Himalayan and sub Himalayan region and a potential of another 300,000, these water mills can lead to a potential power generation of 2500 MW [4].

The problem with the micro hydro power especially in low capacity (Up to 3 kW) is the non availability of the equipment. Generally no standard turbines are available that can be used with a little modification at all the sites. Thus, each site is to be provided with the turbine specifically made for it. Also these turbines are fabricated locally without

much attention being paid to the details. No proper attention is paid for the designing details. This affects the output of the turbine substantially.

1.4 TURBINES SUITABLE FOR MICRO HYDRO RANGE

Hydro turbine is the most important component of a micro hydro power site. Turbines are classified a high head, medium head or low head. Also, they are classified by their working principle and can be classified as impulse or reaction turbine. The general classification is given in Table 1.4

Table 1.4: Classification of Conventional Hydro Turbines based on Head [5]

TURBINES	HIGH HEAD	MEDIUM HEAD	LOW HEAD
Impulse	Pelton Turgo	Cross Flow Multijet Pelton Turgo	Cross Flow
Reaction		Francis	Propeller Kaplan

Also, the turbines are classified by their working principle as

1.4.1 Impulse Turbines

Impulse Turbines use the total available Head of water in the form of Kinetic Energy of one or more jet(s) to run their runners. Movement of water in the runner passage takes place with a free surface contacting the ambient air, which implies that the energy available is extracted from the flow at atmospheric pressure. There is no pressure change across the runner blades. The work is done on the runner by the fluid due to the change in angular momentum and the motion of the vanes. Various types of impulse turbines are discussed below:

1.4.1.1 Pelton Wheel

The modern Pelton wheel is a tangential turbine with discharge buckets as shown in Fig 1.1. In Pelton wheel one or more jets of water impinge on a wheel containing many hemispherical curved buckets. It has a high efficiency of about 90% at the rated output and can maintain same efficiency at part load conditions. It is simple in design and cheap in construction making it more suitable for micro hydro. Pelton turbines are not used at

lower heads because their rotational speed becomes very low. If the runner size and low speed do not pose a problem for particular installation, then pelton turbine can be used efficiently with fairly low heads.

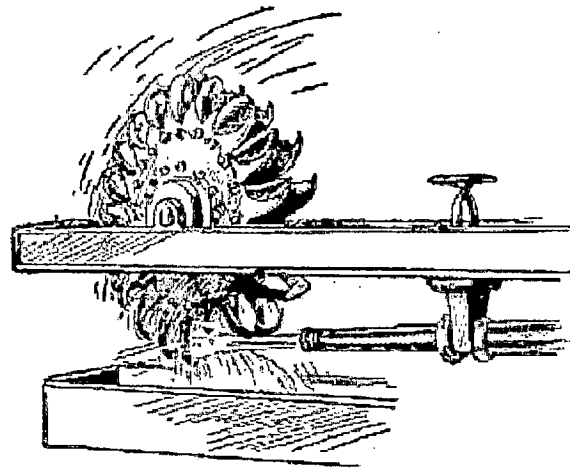


Fig 1.1 A Pelton Wheel [6]

1.4.1.2 Turgo Impulse Turbine

A turgo turbine is an impulse machine similar to the Pelton Wheel but is designed to have a higher specific speed. In this turbine the jet aims to strike the plane of the runner on one side and exit on the other. Therefore, the flow rate is not limited by the discharged fluid interfering with the incoming jet. As a consequence, a turgo turbine can have a smaller diameter runner than the pelton for an equivalent power. With smaller faster spinning runners, it is more likely to be possible to connect turgo turbines directly to the generators rather than having to go via a costly speed increasing transmission [5]. Water impingement on a typical Turgo Runner is shown in Fig 1.2. Turgo Impulse is efficient over wide range of speeds and shares the general characteristics of Impulse Turbines listed for Pelton.

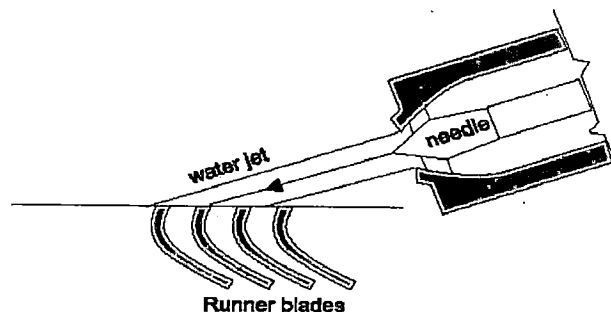


Fig 1.2 Water Impingement on a Turgo Runner [6]

1.4.1.3 Cross Flow Turbines

Cross Flow Turbines are also called 'Michell-Banki' Turbines. It has a drum shaped runner consisting of two parallel discs connected together near the rims by a series of curved blades. A Cross Flow Turbine always has its runner shaft horizontal. Fig 1.3 shows the isometric view of a cross flow runner.

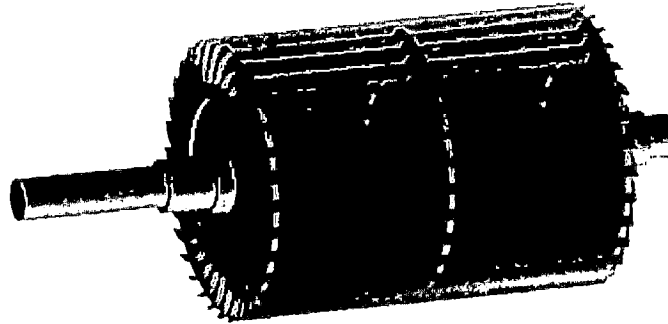


Fig 1.3 Cross Flow Runner [6]

A cross flow turbine consists of following components:

- i) *Nozzle*: for a cross flow turbine the nozzle is of rectangular shape where width matches the width of the runner.
- ii) *Runner*: runner is the central part of the whole turbine. The blades of a cross flow turbine are curved and mounted between two circular discs parallel to the axis of the shaft.
- iii) *Shaft*: the shaft is the integral part of the runner. It transfers the torque generated to the generator or the alternator. A correctly dimensioned shaft allows the jet to the second stage with minimum hindrance.
- iv) *Casing*: Casing is mainly used to prevent the splashing of water and channelize it to the tailrace. However, a small capacity turbine may be without casing which is known as "Open Cross Flow".

In the operation of a Cross Flow Turbine a rectangular nozzle directs the jet onto the full length of the runner. The water strikes the blades and imparts most of its kinetic energy ($2/3$). It then passes through the runner and strikes the blade again on exit, impacting the remaining energy ($1/3$) before leaving the turbine. Although strictly

classified as an impulse turbine, hydrodynamic pressure forces are also involved and a mixed flow definition would be more accurate. High part flow efficiency can be maintained at less than a quarter of full flow. At low flows, the water can be channeled through either two-thirds or one third of the runner, thereby sustaining relatively high turbine efficiency.

The advantages of a Cross Flow turbine are as under:

- Flat Performance Characteristics with respect to change in Head [7]
- Operates under a wide range of flow variations [8]
- It has a maximum achievable efficiency of about 70% [8].
- With a split runner and turbine chamber, the turbine maintains its efficiency while the flow and load vary from 1/6 to the maximum.
- Since it has a low price, and good regulation, cross flow turbines are mostly used in mini and micro hydropower units less than two thousand kW and with heads less than 200 m.
- Due to its excellent behavior with partial loads, the cross flow turbine is well-suited to unattended electricity production.
- Its simple construction makes it easier to maintain than other turbine types; only two bearings must be maintained, and there are only three rotating elements. The mechanical system is simple, so repairs can be performed by local mechanics.
- Another advantage is that it can often clean itself. As the water leaves the runner, leaves, grass etc. will not remain in the runner, preventing losses.

Apart from the above listed advantages the cross flow one major disadvantage that the Cross Flow turbine faces is that Cross flow type runner can be fabricated locally, which results in the degradation of efficiency. The vanes can be made even from the pipes cut along the length. Keeping this in view the present study aims at studying the flow pattern in the cross flow runner so that necessary improvements can be suggested.

1.4.2 Reaction Turbines

In the reaction turbine the energy available at the inlet is pressure energy as well as the Kinetic Energy. The specific speed is quite high for these turbines. Some of the reaction turbines are introduced below.

1.4.2.1 Francis Turbine

Francis Turbine can be either volute cased or open flume machines. The spiral casing is tapered to distribute water uniformly around the entire parameter of the runner. Fig 1.4 shows the runner of Francis Turbine. The guide vanes feed the water into the runner at the correct angle. The Francis Turbine is generally fitted with adjustable guide vanes. These regulate the water flow as it enters the runner and are usually linked to the governing system which matches the flow to turbine loading in the same way as a spear valve or a deflector plate in Pelton Turbine.

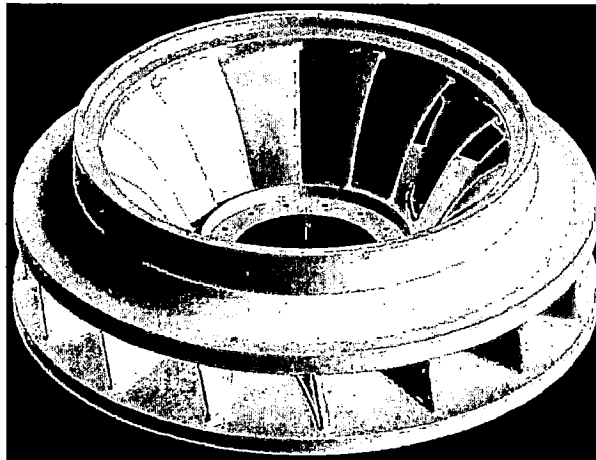


Fig 1.4 The runner of a Francis Turbine [6]

1.4.2.2 Propeller Turbines

The propeller Turbine, which can be used in most of the Axial Flow Turbine configurations. Unfortunately, this simple fixed runner blade, fixed guide vane turbine is only of a limited use, as its efficiency falls off sharply from its nominal operating conditions. However, most of the disadvantages of the simple propeller turbine can be overcome by the use of adjustable blades. The basic propeller turbine consists of a propeller fitted inside the continuation of the penstock tube. The turbine shaft passes out of the tube at the point where the tube changes the direction. The propeller has usually three to six blades and the water flow is regulated by the static blades or swivel gates.

1.5 CONCEPT OF CFD

Computational Fluid Dynamics has emerged as the most efficient and reliable means of studying the turbines. Simulation with the help of CFD based software packages requires comparatively less time and is a good substitute for the actual experimental work required to study the flow. CFD modeling helps in trying different modeling strategies without incurring any additional costs until the desired flow field is obtained and is ready for implementation

1.5.1 Application of CFD

CFD is useful in a wide variety of applications in industry as well as in educational areas. CFD can be used to simulate flow over a vehicle. For instance, it can be used to study the interaction of propellers or rotors with the aircraft fuselage. It can predict the pressure field induced by the interaction of the rotor with a helicopter fuselage in forward flight. Rotors and propellers can be represented with models of varying complexity. It can be used in the various Heat Transfer and flow problems. CFD is attractive to industry since it is more cost-effective than physical testing. However, one must note that complex flow simulations are challenging and error-prone and it takes a lot of engineering expertise to obtain validated solutions.

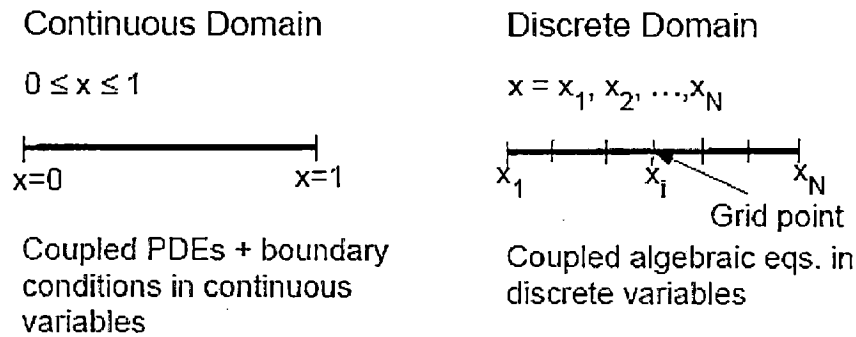
1.5.2 The Strategies of CFD

Broadly, the strategy of CFD is to replace the continuous problem domain with a discrete domain using grid. In the continuous domain, each flow variable is defined at every point in the domain. For instance, the pressure p , in the continuous 1D domain shown in the figure below would be given as

$$p = p(x), 0 < x < 1 \quad (1.1)$$

in the discrete domain, each flow variable is defined only at the grid points. So, in the discrete domain shown below, the pressure would be defined only at the N grid points.

$$p_i = p(x_i), i = 1, 2, \dots, N$$



In a CFD solution, one would directly solve for the relevant flow variables only at the grid points. The values at the other locations are determined by interpolating the values at the grid points. The governing partial differential equations and boundary conditions are defined in terms of continuous variables p , V etc. one can approximate these in the discrete domain in terms of discrete variables p_i , V_i , etc. the discrete system in a large set of coupled algebraic equations in the discrete variables. Setting up the discrete system and solving it (which is a matrix inversion problem) involves a very large number of repetitive calculations and is done by a digital computer.

1.5.3 Discretization Using Finite Volume Method

In the finite volume method the basic quadrilaterals are called 'cells' and a grid point is called as a 'node'. In 2D one can also have triangular cells. In 3D, cells are usually hexahedral, tetrahedral or prisms. In the finite volume method, the integral forms of conservation equations are applied to the control volume defined by a cell to get the discrete equations for the cell. For steady, incompressible flow, this equation is

$$\int_V \hat{n} \cdot dS = 0 \quad (1.2)$$

The integration is over the surface S of the control volume and \hat{n} is the outward normal at the surface. Physically, this equation means that the net volume flow into the control volume is zero. Consider the rectangular cell shown in Fig 1.5.

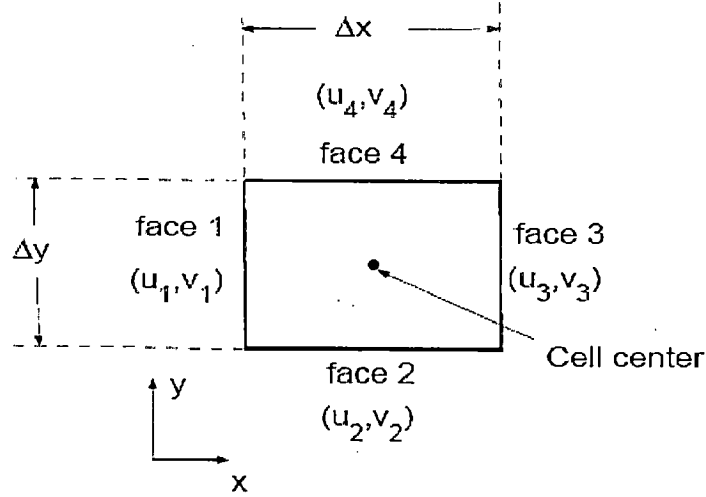


Fig 1.5 Rectangular cell showing faces and cell center [19]

The velocity at face i is taken to be $\vec{V}_i = u_i \hat{i} + v_i \hat{j}$. Applying the mass conservation equation (1.2) to the control volume defined by the cell gives

$$-u_1 \Delta y - v_2 \Delta x + u_3 \Delta y + v_4 \Delta x = 0 \quad (1.3)$$

This is the discrete form of the continuity equation for the cell. It is equivalent to summing up the net mass flow into the control volume and setting it to zero. So it ensures that the net mass flow into the cell is zero i.e. that mass is conserved for the cell. Usually the values at the cell centers are stored. The face values u_1, v_2 , etc. are obtained by suitably interpolating the cell center values for the adjacent cells.

Similarly one can obtain discrete equations for the conservation of momentum and energy for the cell. One can readily extend these ideas to any general cell shape in 2D or 3D and any conservation equation.

1.5.4 Assembly of Discrete System and Application of Boundary Conditions

$$-u_{i-1} + (1 + \Delta x) u_i = 0 \quad (1.5)$$

Applying this equation to the 1D grid shown earlier at grid points $i=2,3,4$ gives

$$-u_1 + (1 + \Delta x) u_2 = 0 \quad (i=2) \quad (1.6)$$

$$-u_2 + (1 + \Delta x) u_3 = 0 \quad (i=3) \quad (1.7)$$

$$-u_3 + (1 + \Delta x) u_4 = 0 \quad (i=4) \quad (1.8)$$

The discrete equation cannot be applied at the left boundary ($i=1$) since u_{i-1} is not defined here. Instead, we use the boundary condition to get

$$u_1 = 1 \tag{1.9}$$

Equations (3.10) – (3.13) form a simple system of four simultaneous algebraic equations in the four unknowns u_1, u_2, u_3, u_4 .

In a general situation, one would apply the discrete; one would apply the discrete equations to the grid points (or cells in the finite volume method) in the interior of the domain. For grid points (or cells) at or near the boundary conditions. In the end, one would obtain a system of simultaneous algebraic equations with the number of equations being equal to the number of independent discrete variables. The process is essentially the same as above with the details being much more complex.

FLUENT offers a variety of boundary condition options such as velocity inlet, pressure outlet etc. It is very important that proper boundary conditions are specified to have a well defined problem.

1.5.5 Direct and Iterative Solvers

Another factor that makes it necessary to carry out iterations in practical CFD problems is the Solvers.

The discrete equation system resulting from the finite difference approximation on the four point grid.

$$\begin{bmatrix} 1 & 0 & 0 & 0 \\ -1 & 1+2\Delta x u_{g2} & 0 & 0 \\ 0 & -1 & 1+2\Delta x u_{g3} & 0 \\ 0 & 0 & -1 & 1+2\Delta x u_{g4} \end{bmatrix} \begin{bmatrix} u_1 \\ u_2 \\ u_3 \\ u_4 \end{bmatrix} = \begin{bmatrix} 1 \\ \Delta x u_{g2}^0 \\ \Delta x u_{g3}^0 \\ \Delta x u_{g4}^0 \end{bmatrix} \tag{1.10}$$

In a practical problem, millions of grid points or cells appear so that each dimension of the above matrix would be of the order of a million (with most elements being zero).

Inverting such a matrix would take a prohibitively large amount of memory. So instead, the matrix is inverted using an iterative scheme as discussed below.

Rearrange the finite difference approximation at the grid point i so that u_i is expressed in terms of the values at the neighboring grid points and the guess values:

$$u_i = \frac{u_{i-1} + \Delta x u_{gi}^2}{1 + 2\Delta x u_{gi}} \quad (1.11)$$

If a neighboring value at the current iteration level is not available, we use the guess value for it. If u_4, u_3, u_2 are updated in that order in each iteration. In the m^{th} iteration, $u_{i-1}^{(l)}$ is not available while updating u_i^m and so we use the guess value $u_{g_{i-1}}^{(l)}$ for it instead:

$$u_i^{(l)} = \frac{u_{g_{i-1}}^{(l)} + \Delta x u_{gi}^{(l)2}}{1 + 2\Delta x u_{gi}^{(l)}} \quad (1.12)$$

Since we are using the guess values at the neighboring points, we are effectively obtaining only an approximate solution for the matrix inversion in (1.10) during each iteration but in the process have greatly reduced the memory required for the inversion. This tradeoff is good strategy since it doesn't make sense to expend a great deal of resources to do an exact matrix elements depend on guess values which are continuously being refined. As the iterations converge and $u_g \rightarrow u$, the approximate solution for the matrix inversion tends towards the exact solution for the inversion since the error introduced by using u_g instead of u in (1.12) also tends to zero.

Thus the iteration serves two purposes:

1. It allows for efficient matrix inversion with greatly reduced memory requirements.
2. It is necessary to solve nonlinear equations.

In steady problems, a common and effective strategy used in the CFD codes is to solve the unsteady form of the governing equations and march the solution in time until the solution converges to a steady value. In this case, each time step is effectively an iteration,

with the guess value at any time level being given by the solution at the previous time level.

1.5.6 Explicit and Implicit Schemes

The difference between explicit and implicit schemes can be most easily illustrated by applying them to the wave equation

$$\frac{\partial u}{\partial t} + c \frac{\partial u}{\partial x} = 0 \quad (1.13)$$

Where c is the wave speed. One possible way to discretize this equation at grid point i and time-level n is

$$\frac{u_i^n - u_i^{n-1}}{\Delta t} + c \frac{u_i^{n-1} - u_{i-1}^{n-1}}{\Delta x} = O(\Delta t, \Delta x) \quad (1.14)$$

The crucial thing to note here is that the spatial derivative is evaluated in the $n-1$ time level n is

$$u_i^n = \left[1 - \left(\frac{c\Delta t}{\Delta x} \right) \right] u_i^{n-1} + \left(\frac{c\Delta t}{\Delta x} \right) u_{i-1}^{n-1} \quad (1.15)$$

This is an explicit expression i.e. the value of u_i^n at any grid point can be calculated directly from an expression without the need of any matrix inversion. The scheme in (1.14) is known as an explicit scheme. Since u_i^n at each grid point can be updated independently, these schemes are easy to implement on the computer. On the downside, it turns out that this scheme is stable only when

$$C \equiv \frac{c\Delta t}{\Delta x} \leq 1 \quad (1.16)$$

Where C is called the Courant number. This condition is referred to as the Courant-Friedrichs-Lewy or CFL condition. While a detailed derivation of the CFL condition through stability analysis is outside the scope of the current discussion, it can be seen that the coefficient of u_i^{n-1} in (1.15) changes sign depending on whether $C > 1$ or $C < 1$ leading to a very different behavior in the two cases. The CFL condition places a rather severe limitation on Δt_{\max} .

In the implicit scheme, the spatial derivative term is evaluated at the n time level.

$$\frac{u_i^n - u_i^{n-1}}{\Delta t} + c \frac{u_i^n - u_{i-1}^n}{\Delta x} = O(\Delta t, \Delta x) \quad (1.17)$$

In this case, u_i^n cannot be updated at each grid point independently. We instead need to solve a system of algebraic equations in order to calculate the values at all grid points simultaneously. It can be shown that this scheme is unconditionally stable so that the numerical errors will be damped out irrespective of how large the time-step is.

The stability limits discussed above apply specifically to the wave equation. In general, explicit schemes applied to the Euler or Navier-Stokes equations have the same restriction that the Courant Number needs to be less than or equal to one. Implicit schemes are not unconditionally stable for the Euler or Navier-Stokes equations since the nonlinearities governing equations often limit stability. However, they allow a much larger Courant number than the Explicit Schemes. The specific value of the maximum allowable Courant Number is problem dependent.

It should be noted that CFD codes allow to set up the Courant Number (which is referred to as CFL number) when using time stepping. Taking larger time steps leads to faster convergence to the steady state, so it is advantageous to set CFL number as large as possible within the limits of stability. It should also be noted that a lower Courant number is required during startup when changes in the solution are highly nonlinear but it can be increased as the solution progresses.

1.6 OBJECTIVE OF THE PRESENT STUDY

As already discussed that besides having several advantages, the cross flow turbine has a disadvantage that since it is used in micro hydro projects with low capacities, not much emphasis is being paid on the design aspect of the turbine. Generally Cross Flow Turbines are manufactured locally which results in the degradation of the performance of the turbine. The vanes can be made by the pipes cut along the length.

The present study aims at performing the flow analysis of a Cross Flow Runner using Computational Fluid Dynamics. The study aims at analyzing the runner with varying shaft diameters and studying their effects on the flow pattern inside the runner.

1.7 LITERATURE REVIEW

Turbine is a very versatile, effective source of electricity and mechanical power. Energy consumption due to Turbines represents a substantial part of the total energy consumption worldwide. The ability to design Turbines with good efficiency and reliability over the whole operating range for a particular application is therefore of great economic significance. Turbines design continually challenges engineers to design, construct, and operate reliable efficient turbines that meets the market needs and respect the environment. With the development of the technology, the demands for the increasing efficiency of turbines are resulting in the great attention being given to more detailed research in the blade design. The flow processes occurring in the Turbines blade rows are very complex. The flow field is three dimensional and unsteady with laminar, transitional and turbulent flow over the blade profiles. The interactions of the flow patterns with the blade boundary layers produce many complex flow features. Numerical models of the full governing equations are, however, expected to capture the details of the complex flow structures in the Turbines. Computational Fluid Dynamics (CFD) has become an increasingly applied and accepted tool in the analysis and design of Turbines. With the advances in algorithms and computer architecture, accurate flow predictions can be performed in a reasonable amount of time. While a sizable simulation can incur a substantial cost in computational resources, a clear understanding of the aerodynamic processes aids the design of Turbines considerably. This thorough comprehension of the entire Turbines flow field can lead to greatly enhanced performance and efficiency. Thus, the computational costs incurred are completely justified. Future designing towards lighter, safer, quieter, and more durable Turbines needs a better understanding of the various unsteady interactions and the mechanism of the effects of these interactions on the Turbines performance. Numerical computation of these unsteady interactions is a very powerful tool in achieving this understanding. In the past twenty years, a lot of computational work has been done on this subject. However, a lot of work still needs to be carried out in terms of validating the unsteady flow code, incorporating more advanced turbulence models, and having the ability to calculate realistic Turbines.

Rajesh Bhaskaran [12], illustrated the basic concepts of CFD by applying them to simple 1D example and applications of CFD techniques to the most of engineering problems. The discretization using the finite difference method, finite volume method, assembly of discrete system and application of boundary conditions and the solution has been explained. Dealing with non-linearity occurred in simulation.

Suhas V. Patankar [10] presented various numerical methods to develop numerical equations for the fluid flow and heat transfer. He also discussed the various methods of discretization equations and presented the algorithm to solve pressure correction equations like SIMPLER which is revised as SIMPLE from which the forces acting at each grid point can be derived.

John D. Anderson junior [11] explained the basic equations required to apply the CFD for various problems occurring in the common practice like flow behavior in the turbo machines, flow over airplane wings and heat transfer. He discussed the step by step procedure on developing the mathematical equations and mentioned the different methods used for solving the mathematical equations applied in CFD like SIMPLE and SIMPLER.

Balint D et al [13], mentioned the numerical simulation of the three dimensional flows in hydraulic turbines is established as one of the main tools in design, analysis and the optimization of turbo machines. A methodology for completing the 3D inviscid flow in Kaplan turbines has been presented. Both velocity and pressure field results are presented with a particular focus on the runner blades pressure distribution.

Ernest C. Perry [14], A Doctorate thesis submitted to the Brigham Young University, develops a new method for three dimensional shape optimization of fluid flow in internal fluid flows. It solves two of the major obstacles associated with three dimensional shape optimization. The first is the current lack of general methodology for parameterization of three dimensional shapes. The second is the absence of the method to manipulate the shape of the analysis model while maintaining its ability to produce

accurate results. This method called arbitrary shape deformation is similar to lattice deformation methods currently used in the field of computer graphics.

Numerical study of flow and heat transfer in Turbo machinery, A dissertation submitted by Cheng Xu to the university of Wisconsin Milwaukee [15]. The study develops an accurate and efficient CFD code for turbo machinery flow and Heat Transfer problems. The study presents three related code developments: A Two-Dimensional time marching Navier Stokes code, a quasi three dimensional code, and a three dimensional code. Stokes equation was developed to simulate turbine cascade flow and heat transfer problems. The overall difference scheme consists of an explicit step in global time steps and an implicit step in local time steps. The numerical method proposed in this study comprises of positive features of both implicit and explicit schemes.

Structured and Unstructured Computations of unsteady Turbo machinery flows using pressure based methods, A Thesis submitted by Wen-Sheng Yu [16] to the Pennsylvania State University. The thesis aims at an improved understanding of unsteady turbo machinery flow physics using time accurate Computational Fluid Dynamic Techniques. Two pressure based algorithms were adopted for the numerical computations of turbulent, Two and Three dimensional, steady and Unsteady flows through turbo machines. The differential model employed was the incompressible Reynolds' average Navier-Stokes equation. In this study several new and modern techniques have been adopted, implemented and applied. These include higher order accurate structured and hybrid unstructured discretization, an inlet wake passing strategy, an interface sliding technique for the computations of rotor stator interactions, parallel processing capability, and full two fluid modeling for multiphase flow analysis. The methods are employed in the analysis of several unsteady turbo machinery flows. The results are presented compared with experimental data and interpreted, elucidating several important intrinsically unsteady flows in these machines.

Parametric Study on the performance of Cross Flow Turbine, C.B. Joshi, V. Sheshadri and S.N. Singh [7]. In this Experimental study the effects of blades number,

nozzle entry arc, and the head on the performance characteristics of a cross flow turbine have been investigated. It was observed that the efficiency of the turbine increases with the increase in blade number, Head and nozzle entry arc. The study also shows that there is an optimum value for the number of blades for a given nozzle entry beyond which the performance of cross flow turbine deteriorates. This paper also shows that the cross flow turbines with high heads do not behave as pure impulse turbines.

Khosrowpanah S, (1984) [17], Experimental Study of cross flow turbine, The performance of the cross-flow turbine, CFT, also known as the Banki turbine, was studied experimentally by varying the number of blades, the runner diameter, and the nozzle entry arc under flow-head variations. The results, as presented in this paper, show that the maximum efficiency of the CFT at any flow/head combination increases as the nozzle entry arc increases or the aspect ratio of the runner decreases. Equations have been suggested to obtain the optimum number of blades for maximum efficiency of the turbine and to find the specific speed of the CFT as a function of unit discharge and nozzle entry arc.

Desai, Vengappayya Rangappayya [18], A Parametric Study of Cross Flow Turbine Analysis, A Thesis submitted to Clemson University. This study is an experimental investigation of the key parameters influencing the turbine efficiency and a theoretical analysis of turbine performance. One physical parameter (flow rate) and six geometric parameters (angle of water entry, diameter ratio, number of blades, flow stream spreading, runner aspect ratio, and blade exit angle) are identified as key parameters for the study. A total of 39 runners and 11 nozzles were tested in 75 different combinations. The experimental investigation included measurements of torque, speed, flow rate, and total head in physical models of turbine and nozzles. The theoretical analysis was based on the principles of dynamics and resulted in a simplified linear relationship between the shaft torque and speed. The results indicate that theoretical analysis can be used only as a preliminary predictive technique for maximum turbine efficiency, as verified by the experimental data. Multiple regression and probability analyses are performed to quantify the impact of the parameters on the cross-flow turbine

efficiency. Other techniques such as uncertainty analysis, sensitivity analysis, confidence limit analogy, and critical path method analogy are used to interpret the accuracy of the results. For the best nozzle-runner combination, the maximum efficiency closest to the discharge averaged maximum efficiency is determined to be 88.0% with an uncertainty of $\pm 2.4\%$, which is an improvement over the claimed maximum efficiency reported in the literature. The analysis of the experimental data clearly identifies parametric ranges in which efficiency can be improved. These results suggest that by careful choice of design parameters, the cross-flow turbine can be made as efficient as other traditional turbines; yet has the advantage of low cost and simple structure.

FLUENT Documentation [25], [26] provides all the necessary help to understand and execute the software.

CHAPTER 2

DESIGN OF CROSS FLOW TURBINE RUNNER

2.1 GENERAL

As discussed in the earlier chapter, the Cross Flow Turbine is mostly suitable for micro hydro power plants. These plants have the capacity ranging from 5 to 10 kW. The reason why Cross Flow Turbine is suitable for these applications is that these turbines have low price, good regulation, excellent behavior with part loads, simple in construction and easy maintenance. In this chapter a turbine having 5 kW capacity has been designed and discussed.

2.2 SIZING OF THE TURBINE

2.2.1 Site Data [1]

A typical site having following specifications has been considered for the design of Cross Flow Turbine.

Design Head = 8.0 m

Design Discharge = 0.150 m³/s

Taking turbine Speed = 400 rpm

2.2.2 Steps of Design

Following are the steps in the design of a cross flow turbine runner.

2.2.2.1 Blade Geometry

Before moving on to the Design of the turbine, it is important to understand the geometry of the blade shown in Fig 2.1 and the various parameters are

R_1 is the outer radius of the runner

R_2 is the inner radius of the runner, locus at the end of the skeleton lines of the blades

β_1 is the outer blade angle

β_2 is the inner blade angle

r_b is the curvature radius of the blade

r_p is the pitch circle radius

δ is the segment angle of the blade

the following expressions are listed in the required order for calculating the parameters δ , r_p , r_b , based on the parameters $R_1, R_2, \beta_1, \beta_2$.

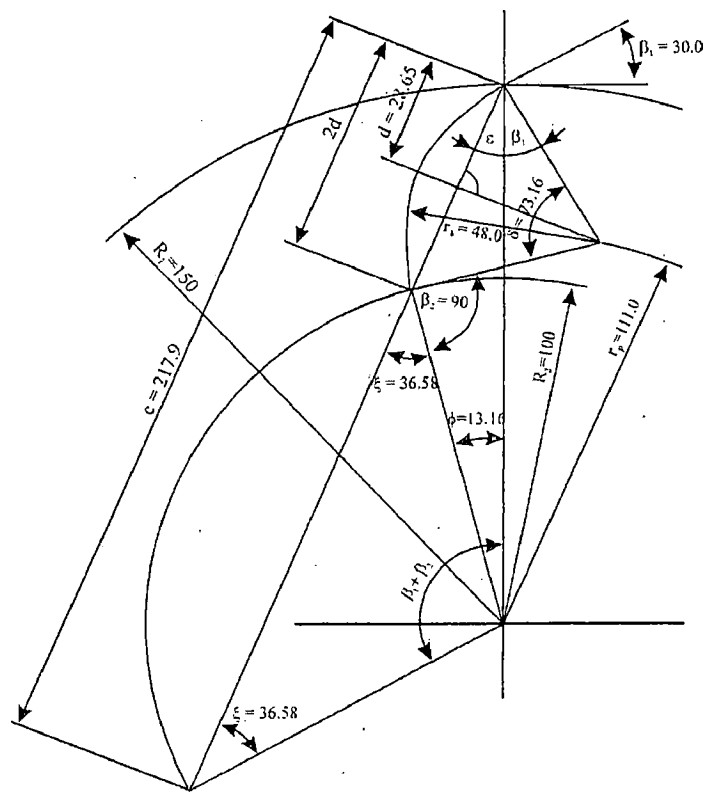


Fig 2.1 Geometry of Blades of Cross Flow Turbine

$$\phi = \beta_1 + \beta_2 - (180 - 2\xi) \quad (2.1)$$

$$\delta = \frac{R_1 \sin \phi}{2 \sin(180 - 2\xi)} \quad (2.2)$$

$$\delta = 180^\circ - 2(\beta_1 + \varepsilon) \quad (2.3)$$

$$r_b = \frac{d}{\cos(\beta_1 + \varepsilon)} \quad (2.4)$$

$$r_b = \sqrt{r^2 + R_1^2 - 2r_b R_1 \cos \beta_1} \quad (2.5)$$

The logarithmically spiral is expressed by the formula:

$$r_\phi = e^{k\phi} \quad (2.7)$$

$$K = \cot k \quad (2.8)$$

($k > 0$)

Where,

r_ϕ = the distance of a point on the angle from the origin

e = the natural logarithm

K = Cotangent of the angle between the tangent to the logarithmically spiral and its radius vector to the origin of the spiral = $\tan \alpha_1$.

ϕ = the angle expressed in radians between two points on the spiral and the origin of the spiral.

Equation below represents all the relevant parameters, influencing the discharge through the turbine. The flow admission area of a cross flow turbine is shown in fig.

$$Q = \frac{b_0 2R_1 \pi \phi^\circ \sqrt{2gH}}{360^\circ} \sin \alpha \quad (2.9)$$

where,

b_0 is the inlet width

R_1 the radius or diameter $D = 2R_1$ the runner

ϕ° is the admission arc angle

H is the net head

$\sin \alpha$ is the sin of the absolute velocity angle at the entrance to the runner.

2.2.2.2 Design for the given data

The procedural Steps for the design of the given data are as under

Diameter of the runner = 300 mm

$$\begin{aligned} \text{i.e } R_1 &= 150 \text{ mm} \\ \text{and } R_2 &= 0.666 R_1 = 100 \text{ mm} \end{aligned}$$

For determining blade geometry other parameters required are calculated as;

$$C = \sqrt{R_1^2 + R_2^2 - 2R_1R_2 \cos(\beta_1 + \beta_2)} \quad (2.10)$$

Taking $\beta_1 = 30^\circ$ and $\beta_2 = 90^\circ$

$$\therefore C = \sqrt{150^2 + 100^2 - 2 * 150 * 100 \cos(30 + 90)} = 217.9 \text{ mm}$$

$$\varepsilon = \text{Sin}^{-1} \left[\frac{R_2 \sin(\beta_1 + \beta_2)}{C} \right] \quad (2.11)$$

$$= \text{Sin}^{-1} \left[\frac{100 \sin(30 + 90)}{217.9} \right]$$

$$= 23.42^\circ$$

$$\xi = 180 - (\beta_1 + \beta_2 + \varepsilon) \quad (2.12)$$

$$= 180 - (30 + 90 + 23.42) = 36.58^\circ$$

$$\phi = \beta_1 + \beta_2 - (180 - 2\xi) \quad (2.13)$$

$$= 30 + 90 - (180 - 2 * 36.58) = 13.16^\circ$$

$$d = \frac{R_1 \sin \phi}{2 \sin(180 - \xi)} \quad (2.14)$$

$$= \frac{150 \sin(13.16)}{2 \sin(180 - 36.56)}$$

$$\delta = 180 - 2(\beta_1 + \varepsilon) \quad (2.15)$$

$$= 180 - 2(30 + 23.42) = 73.16$$

$$r_b = \frac{d}{\cos(\beta_1 + \varepsilon)} \quad (2.16)$$

$$= \frac{28.65}{\cos(30 + 23.42)} = 48.0 \text{ mm}$$

$$r_p = \sqrt{r_b^2 + R_1^2 - 2r_b R_1 \cos \beta_1} \quad (2.17)$$

$$= \sqrt{48^2 + 150^2 - 2 * 48 * 150 * \cos 30} = 111.0 \text{ mm}$$

Check for the flow rate

$$Q = \frac{b_o 2R_1 \pi \phi^0 \sqrt{2gH}}{360^\circ} \sin \alpha \quad (2.18)$$

$$= \frac{0.200 * 2 * 0.150 * \pi * 90^\circ \sqrt{2 * 9.81 * 8 \sin 16}}{360^\circ} = 0.162 \text{ m}^3/\text{s}$$

The same runner diameters under low head say about 5.0 m; let us take runner width as 300 mm.

Flow admission area can be checked for this condition as;

$$A = b_o L \quad (2.19)$$

Where, b_o is the inlet width

L_1 is the admission arc length

$$L = \frac{2R_1 \pi \phi}{360^\circ} \quad (2.20)$$

$$= \frac{2 * 0.150 * \pi * 90}{360^\circ} = 0.2356 \text{ m}$$

$$A = \frac{Q}{C_m} \quad (2.21)$$

Where, Q is taken as 200 lps for 5.0 kW output under 5.0 m head.

$$\text{And } C_m = \sqrt{2gH \sin \alpha} \quad (2.22)$$

$$= \sqrt{2 * 9.81 * 5 \sin 16} = 2.73 \text{ m/s}$$

$$\text{and, } A = \frac{Q}{C_m} = \frac{0.20}{2.73} = 0.0732 \text{ m}^2$$

$$b_o = \frac{A}{L} = \frac{0.0732}{0.2356} = 0.310, \text{ say } 300 \text{ mm} \quad (2.23)$$

CHAPTER 3

MODELING, MESHING AND THE SOLVER

3.1 GENERAL

In the previous chapter 2 sizing of runner and profile has been discussed for a typical site. In order to carry out the CFD for the designed runner, modeling, meshing and analysis required for the analysis has been presented under this chapter.

As it was discussed that the cross flow runner is a two-stage runner. Most of the energy is transferred to the runner at 1st stage and remaining, about $1/3^{\text{rd}}$ is transferred at stage II. Water jet enters at the periphery of the runner, flows over the blade radially, crosses the shaft and then enters the runner blade at stage II. It is observed that the shaft may disturb the flow path between stage I and Stage II. Thus, there is a scope to study the flow characteristics with respect to the shaft thickness. Under the present study modeling has been carried out by varying the shaft thickness of a cross flow runner.

3.2 SOLID MODELLING

The first step in the present analysis was to develop a model of the blade which needs to be analyzed. This is done by the solid modeling of the blade with the help of blade geometry as the basic requirement.

Solid modeling is the unambiguous representation of the solid parts of an object, that is, models of solid objects suitable for computer processing. It is also known as volume modeling.

Solid modeling software creates a virtual 3D representation of components for machine design and analysis. Interface with the human operator is highly optimized and includes programmable macros, keyboard shortcuts and dynamic model manipulation. The ability to dynamically re-orient the model, in real-time shaded 3D, is emphasized and helps the designer maintain a mental 3D image. Design work on components is usually done within context of the whole product using assembly modeling methods.

A solid model generally consists of a group of features, added one at a time, until the model is complete. Engineering solid models are built mostly with sketcher-based

features; 2D sketches that are swept along a path to become 3D. These may be cuts or extrusions for example.

Engineering drawings are created semi-automatically and reference the solid models. The learning curve for these software packages is steep, but a fluent machine designer who can master these software packages is highly productive. The modeling of solids is only the minimum requirement of a CAD system's capabilities. Parametric modeling uses parameters to define a model (dimensions, for example). The parameter may be modified later, and the model will update to reflect the modification. Typically, there is a relationship between parts, assemblies, and drawings. A part consists of multiple features, and an assembly consists of multiple parts. Drawings can be made from either parts or assemblies. Related to parameters, but slightly different are Constraints. Constraints are relationships between entities that make up a particular shape. For a window, the sides might be defined as being parallel, and of the same length. Parametric modeling is obvious and intuitive. But for the first three decades of CAD this was not the case. Modification meant re-draw, or add a new cut or protrusion on top of old ones. Parametric modeling is very powerful, but requires more skill in model creation. A complicated model for an injection molded part may have a thousand features, and modifying an early feature may cause later features to fail. Skillfully created parametric models are easier to maintain and modify. Parametric modeling also lends itself to data re-use.

The basic requirement for the modeling is the geometry of the blade which is defined as under.

3.2.1 Pro/ENGINEER

The modeling has been done on the CAD software Pro Engineer. Pro/ENGINEER is a solid modeler—it develops models as solids, allowing us to work in a three-dimensional environment. Pro/ENGINEER is a suite of programs that are used in the design, analysis, and manufacturing of a virtually unlimited range of products. In Pro/ENGINEER,

- The solid models have volumes and surface areas.
- We can calculate mass properties directly from the geometry we create.

- While we can manipulate a solid model's display on the screen, the model itself remains a solid.
- As a solid modeling tool, Pro/ENGINEER is feature-based, associative, and parametric.

3.2.1.1 Properties of Pro/ENGINEER

Following are the properties of Pro/ENGINEER that makes it user friendly and important software to work upon

i) Feature-Based

Pro/ENGINEER is feature-based. Geometry is composed of a series of easy to understand features. A feature is the smallest building block in a part model. Things to remember:

- Pro/ENGINEER allows building a model incrementally, adding individual features one at a time.
- This means, as you construct your model feature by feature you choose your building blocks as well as the order you create them in, thus capturing your design intent.
- Design intent is the motive, the all-driving force, behind every feature creation.
- Simple features make your individual parts as well as the overall model flexible and reliable.

ii) Parametric

Pro/ENGINEER is parametric i.e. it is driven by parameters or variable dimensions.

This means:

- Geometry can be easily changed by modifying dimensions
- Features are interrelated.
- Modifications of a single feature propagate changes in other features as well, thus preserving design intent.
- A relationship, known as a parent/child relationship, is developed between features when one feature references another.

iii) Associative

Pro/ENGINEER models are often combinations of various parts, assemblies, drawings, and other objects. Pro/ENGINEER makes all these entities fully *associative*.

That means if you make changes at a certain level those changes propagate to all the levels. For example if you change dimensions on a drawing the change will be reflected in the associated part.

3.2.2 Blade Profile

As discussed earlier in chapter two, the blade of a cross flow runner has a particular geometry. This geometry is developed on Pro/ENGINEER and is shown in Fig 3.1.

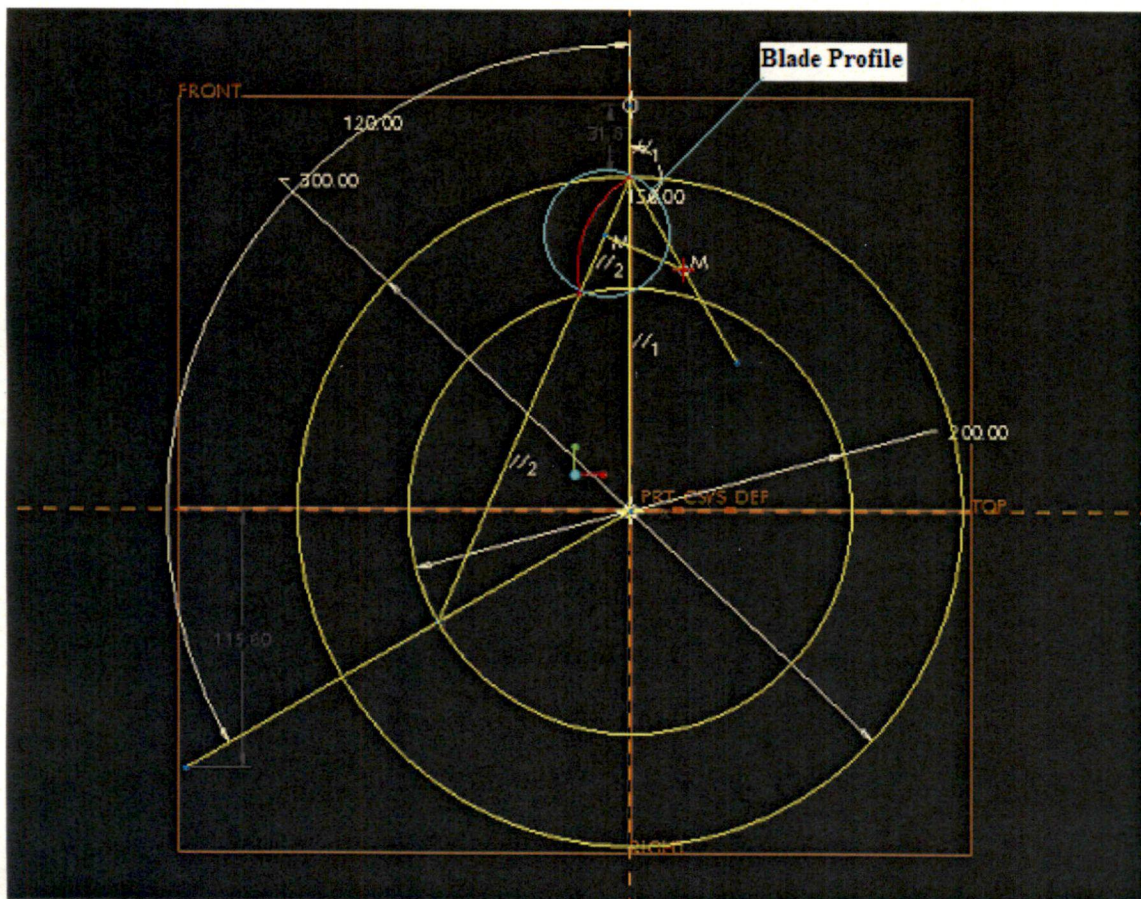


Fig 3.1 The Blade Geometry as drawn on Pro-Engineer

The Profile of the blade is shown in Fig 3.1. After the blade geometry is final it is extruded to give the length of 300 mm which is the length of the blade. Fig 3.2 shows the general view of the extruded blade.

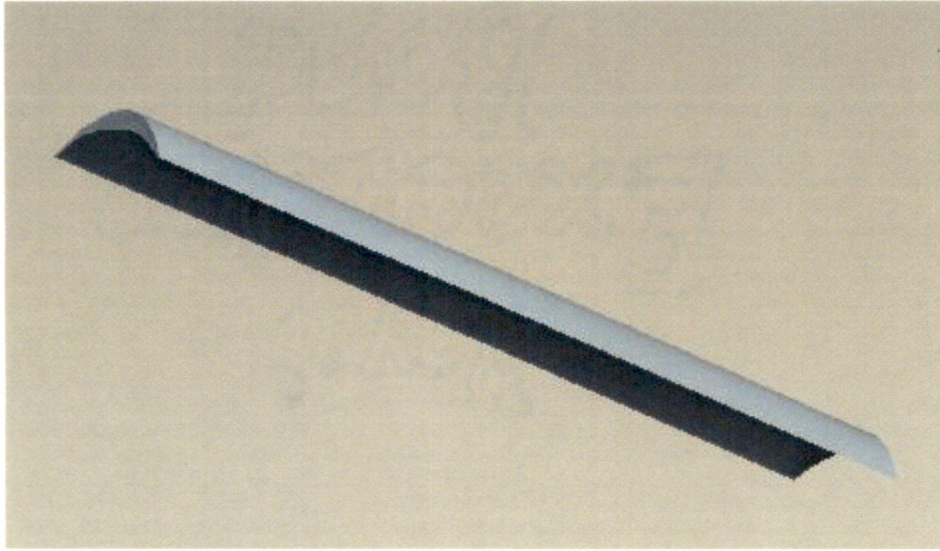


Fig 3.2 General view of the extruded blade

After the completion of the profile of the blade the next step is to make the model of the portion of the runner i.e. the blades that are coming under the nozzle. The nozzle covers an angle of 90° . The number of blades considered for the case is 22. So, every blade is at an angle of 16.3637° from the centre of the runner. The modeling of the runner is done in GAMBIT, which is discussed under the meshing section.

3.3 MODELING OF CROSS FLOW TURBINE RUNNER

Following the step of modeling discussed above the modeling of cross flow runner has been carried out under different conditions of varying diameters of the through shafts. The different values of the diameters of shaft considered are 50.8 mm, 38.1 mm, 25.4 mm and 12.7 mm. Fig 3.3, Fig 3.4, Fig 3.5, Fig3.6 Fig 3.7 show the model of the portion of runner below the nozzle with varying shaft diameters. Fig 3.8 shows the full runner modeled with a through shaft of diameter 50.8 mm.

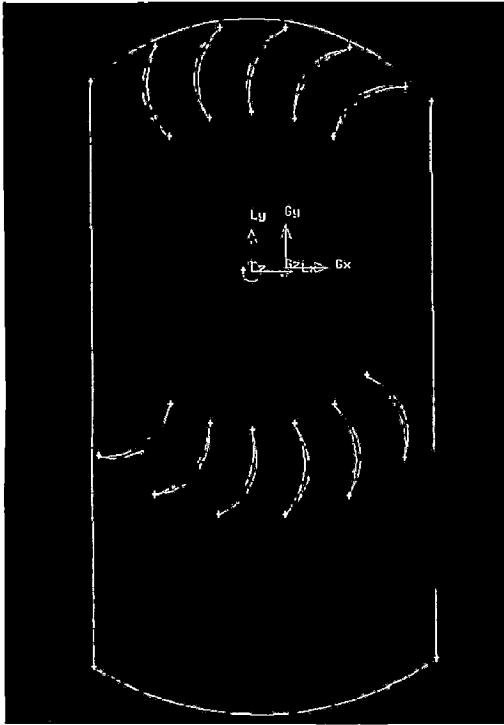


Fig 3.3 Shaft diameter of 12.7 mm

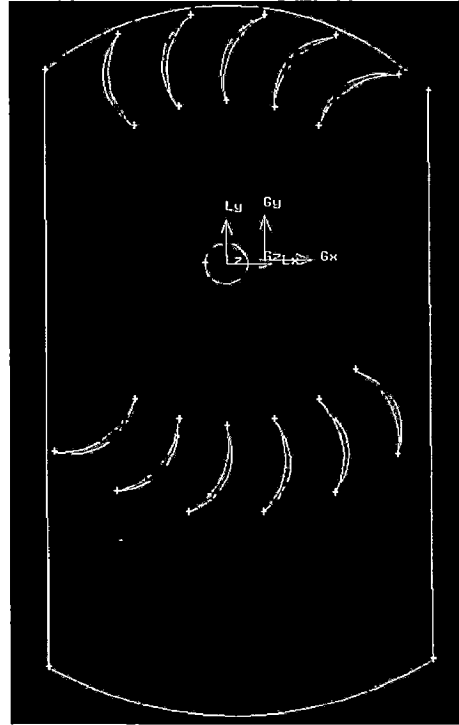


Fig 3.4 Shaft diameter of 25.4 mm

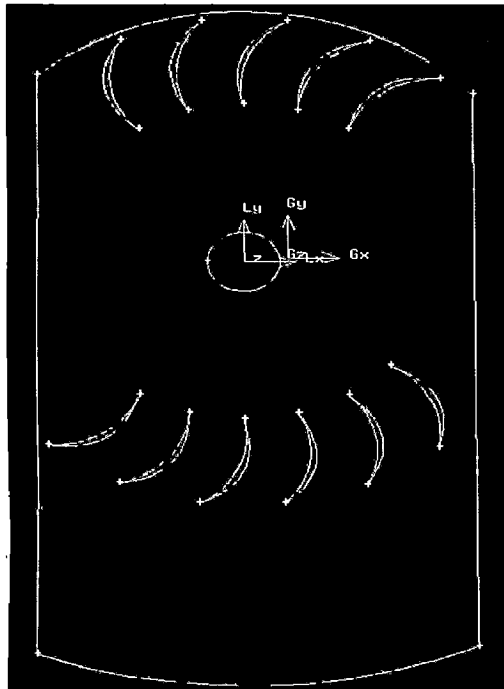


Fig 3.5 Shaft diameter of 38.1 mm

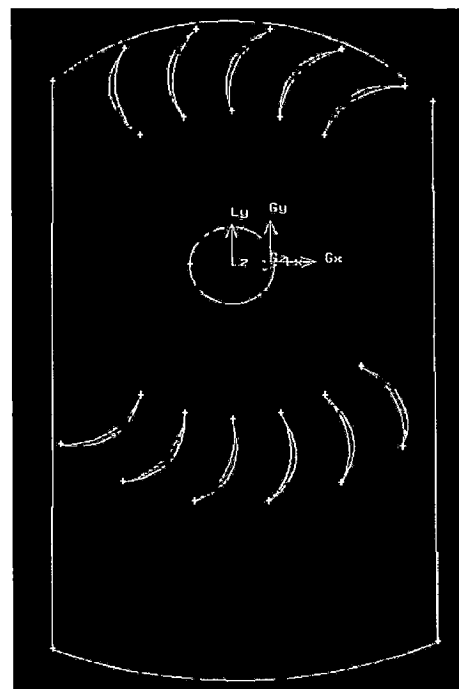


Fig 3.6 Shaft diameter 50.8 mm

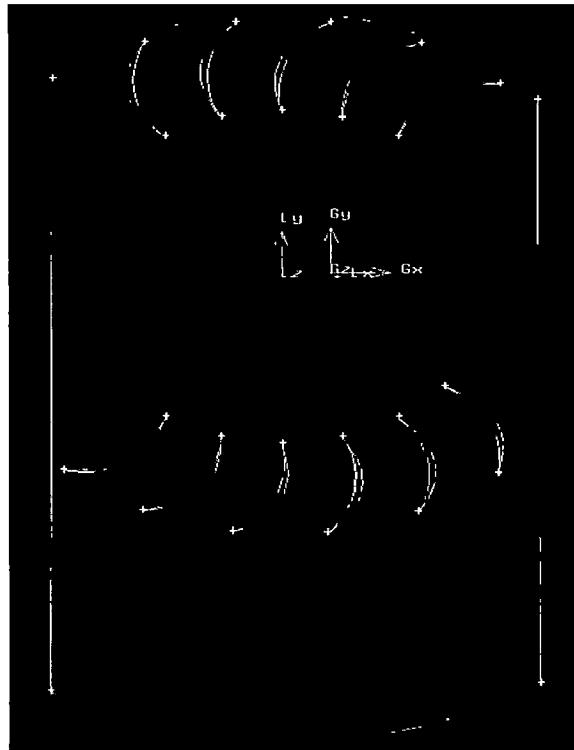
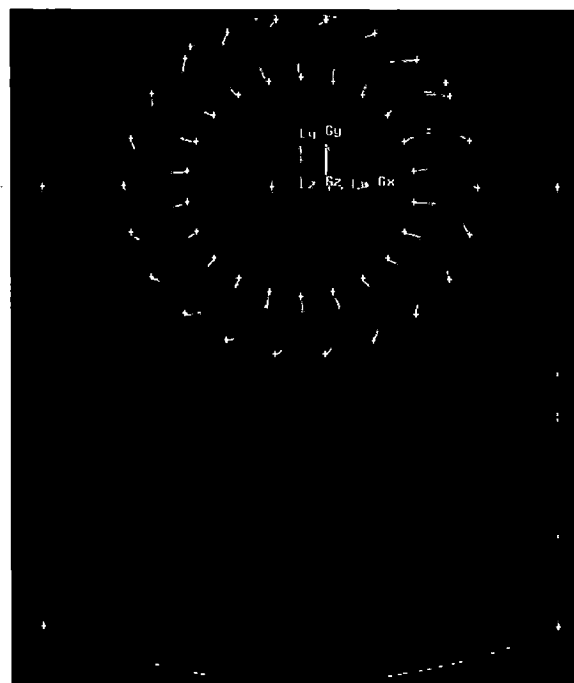


Fig 3.7 Model of runner with no shaft



**Fig 3.8 Model of Full Runner with
Shaft diameter of 50.8 mm**

3.4 MESHING

The partial differential equations that govern fluid flow and heat transfer are not usually amenable to analytical solutions, except for very simple cases. Therefore, in order to analyze fluid flows, flow domains are split into smaller sub domains (made up of geometric primitives like hexahedra and tetrahedral in 3D and quadrilaterals and triangles in 2D). The governing equations are then discretized and solved inside each of these sub domains. Typically, one of three methods is used to solve the approximate version of the system of equations: finite volumes, finite elements, or finite differences. Care must be taken to ensure proper continuity of solution across the common interfaces between two sub domains, so that the approximate solutions inside various portions can be put together to give a complete picture of fluid flow in the entire domain. The sub domains are often called elements or cells, and the collection of all elements or cells is called a mesh or grid. The origin of the term mesh (or grid) goes back to early days of CFD when most analyses were 2D in nature. For 2D analysis, a domain split into elements resembles a wire mesh, hence the name.

The process of obtaining an appropriate mesh (or grid) is termed mesh generation (or grid generation), and has long been considered a bottleneck in the analysis process due to the lack of a fully automatic mesh generation procedure. Specialized software programs have been developed for the purpose of mesh and grid generation, and access to a good software package and expertise in using this software are vital to the success of a modeling effort.

As CFD has developed, better algorithms and more computational power has become available to CFD analysts, resulting in diverse solver techniques. One of the direct results of this development has been the expansion of available mesh elements and mesh connectivity (how cells are connected to one another). The easiest classifications of meshes are based upon the connectivity of a mesh or on the type of elements present.

3.4.1 Connectivity-Based Classification

The most basic form of mesh classification is based upon the connectivity of the mesh: structured or unstructured.

3.4.1.1 Structured Meshes

A structured mesh is characterized by regular connectivity that can be expressed as a two or three dimensional array. This restricts the element choices to quadrilaterals in 2D or hexahedra in 3D. The above example mesh is a structured mesh, as we could store the mesh connectivity in a 40 by 12 array. The regularity of the connectivity allows us to conserve space since neighborhood relationships are defined by the storage arrangement. Additional classification can be made upon whether the mesh is conformal or not.

3.4.1.2 Unstructured Meshes

An unstructured mesh is characterized by irregular connectivity is not readily expressed as a two or three dimensional array in computer memory. This allows for any possible element that a solver might be able to use. Compared to structured meshes, the storage requirements for an unstructured mesh can be substantially larger since the neighborhood connectivity must be explicitly stored.

3.4.1.3 Hybrid Meshes

A hybrid mesh is a mesh that contains structured portions and unstructured portions. Note that this definition requires knowledge of how the mesh is stored (and used). There is disagreement as to the correct application of the terms "hybrid" and "mixed." The term "mixed" is usually applied to meshes that contain elements associated with structured meshes and elements associated with unstructured meshes (presumably stored in an unstructured fashion).

3.4.2 Element-Based Classification

Meshes can also be classified based upon the dimension and type of elements present. Depending upon the analysis type and solver requirements, meshes generated could be 2-dimensional (2D) or 3-dimensional (3D). Common elements in 2D are triangles or rectangles, and common elements in 3D are tetrahedral or bricks. As noted above, some connectivity choices limit the types of element present, so there is some overlap between connectivity-based and element-based classification.

For a 2D mesh, all mesh nodes lie in a given plane. In most cases, 2D mesh nodes lie in the XY plane, but can also be confined to another Cartesian or user defined plane. Most popular 2D mesh elements are quadrilaterals and triangles

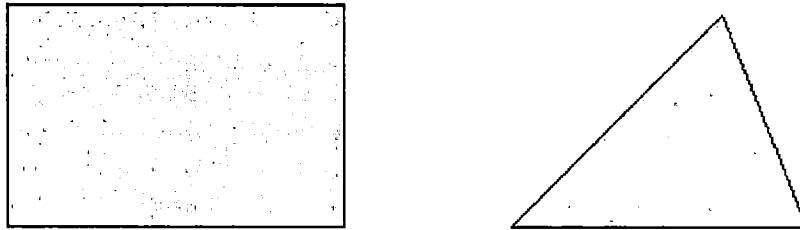


Fig 3.9: 2D Quadrilateral and Triangular Mesh Elements

3D mesh nodes are not constrained to lie in a single plane. Most popular 3D mesh elements are hexahedra (also known as hexes or hex elements), tetrahedra (tets), square pyramids (pyramids) and extruded triangles (wedges or triangular prisms), shown below. It is worth noting that all these elements are bounded by faces belonging to the above mentioned 2D elements. Some of the current solvers also support polyhedral elements, which can be bounded by any number and types of faces.

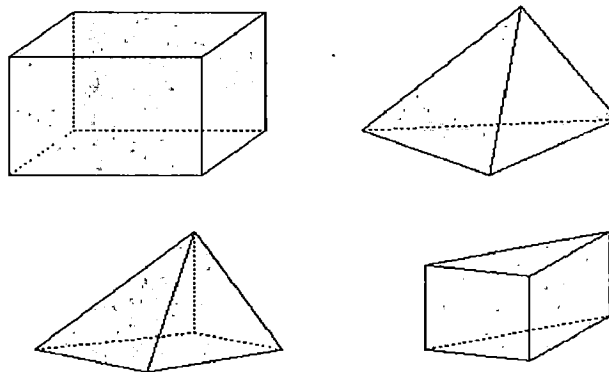


Fig 3.10 3D Hexahedra, Tetrahedra and Triangular Prism Mesh Elements

Since all 3D elements are bounded by 2D elements, it is obvious that 3D meshes have exposed 2D elements at boundaries. Most of the meshing packages and solvers prefer to club exposed elements together in what is known as a surface mesh (for the purposes of applying boundary conditions, rendering meshed domains and visualizing results). A surface mesh does not have to be 2D, since volume meshes may conform to domains with non-planar boundaries. Many meshing algorithms start by meshing bounding surfaces of a domain before filling the interior with mesh nodes (such algorithms are also known as boundary to interior algorithms). For such algorithms, generation of good quality surface meshes is of prime importance, and much research has been done in the field of efficient and good quality surface mesh generation. Since surface meshes are geometrically somewhere between 2D and 3D meshes, they are also sometimes known as 2.5D meshes.

3.4.3 MESHING OF CROSS FLOW RUNNER

Following the steps discussed earlier, the meshing of the cross flow runner with varying shaft diameter is carried out.

3.4.3.1 GAMBIT

The meshing of the present model has been done on the software GAMBIT. GAMBIT is Fluent's geometry and mesh generation software. GAMBIT's single interface for geometry creation and meshing brings together most of Fluent's preprocessing technologies in one environment. Advanced tools for journaling let you edit and conveniently replay model building sessions for parametric studies. GAMBIT's combination of CAD interoperability, geometry cleanup, decomposition and meshing tools results in one of the easiest, fastest, and most straightforward preprocessing paths from CAD to quality CFD meshes.

As a state-of-the-art preprocessor for engineering analysis, GAMBIT has several geometry and meshing tools in a powerful, flexible, tightly-integrated, and easy-to use interface. GAMBIT can dramatically reduce preprocessing times for many applications. Most models can be built directly within GAMBIT's solid geometry modeler, or imported

from any major CAD/CAE system. Using a virtual geometry overlay and advanced cleanup tools, imported geometries are quickly converted into suitable flow domains. A comprehensive set of highly automated and size function driven meshing tools ensures that the best mesh can be generated, whether structured, multi block, unstructured, or hybrid. GAMBIT's range of CAD readers allow you to bring in any geometry, error free, into its meshing environment. GAMBIT also has an excellent boundary layer mesher for growing optimum grid cells off wall surfaces in your geometries for fluid flow simulation purposes. The model of the blade which is made in Pro-E is saved in .iges format which is imported to GAMBIT for further modeling. GAMBIT has a default coordinate system known as global coordinate system but for producing our runner a new coordinate system was required. This coordinate system which is called the Local Coordinate system is made which is Cartesian in nature and location and orientation is defined by vertices. After we have the local coordinate system the edges of the imported geometry are joined to form a face. Taking the center of the local coordinate system as the center of the runner the blades are reproduced at an angle of 16.3637° from every adjacent blade. Thus, in all four blades are present in the top side and five on the bottom side. Then, nozzle is made and also a computational domain which is required for the calculations. Once the entire calculating domain is made, the model has to be edited a little for the meshing. The entire computational domain is defined as one face and blades and shaft as different faces. In the face tab we have an option of subtraction from where blades and shaft are subtracted from the first face. Thus, the runner model is now ready to be meshed. Various runner models with varying diameter of shaft are shown below. The model of the runner which is now ready to be meshed is opened in GAMBIT. The option of face mesh is activated. After subtraction there is only one face that has to be meshed. This face is selected and since the geometry has sharp corners and irregularity, triangular element is selected. Spacing is given by an interval count of 100. A large value of interval count is taken because the mesh will be finer and calculations will be more accurate. The runner is now meshed. Figs 3.11, 3.12, 3.13, 3.14,3.15, show the meshed models with varying diameters of the shafts. Fig 3.16 shows the meshed model of the full runner with shaft diameter of 50.8 mm.

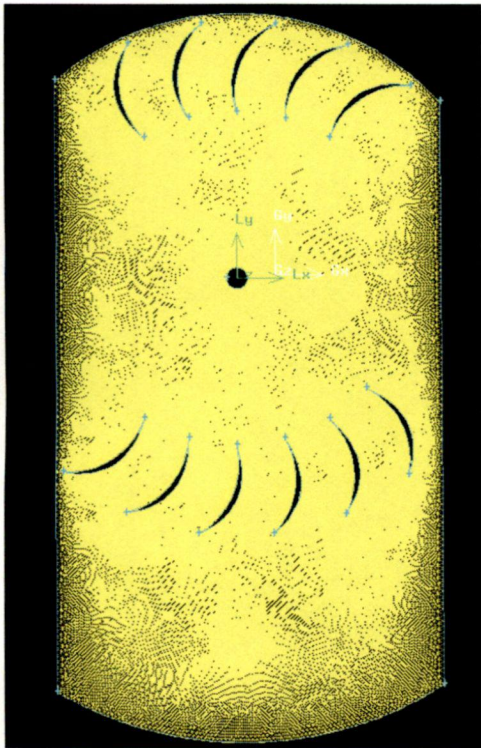


Fig 3.11 Meshed Model (12.7 mm)



Fig 3.12 Meshed Model (25.4 mm)



Fig 3.13 Meshed Model (38.1 mm)



Fig 3.14 Meshed Model (50.8 mm)

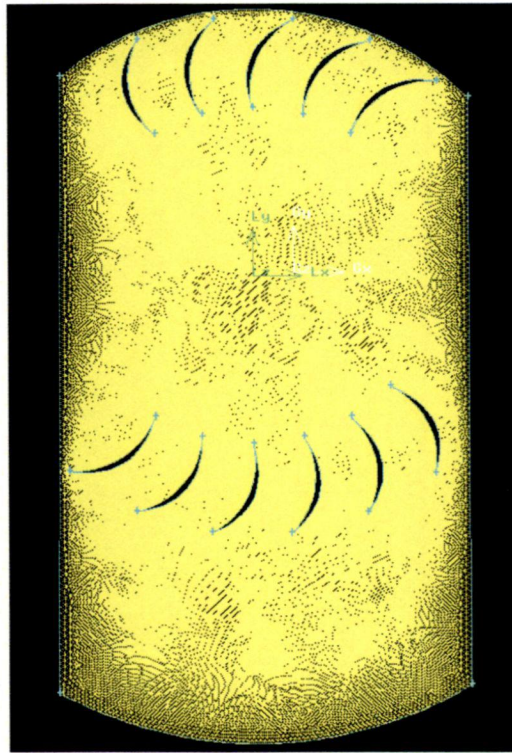


Fig 3.15 Meshed Model of Runner with no shaft

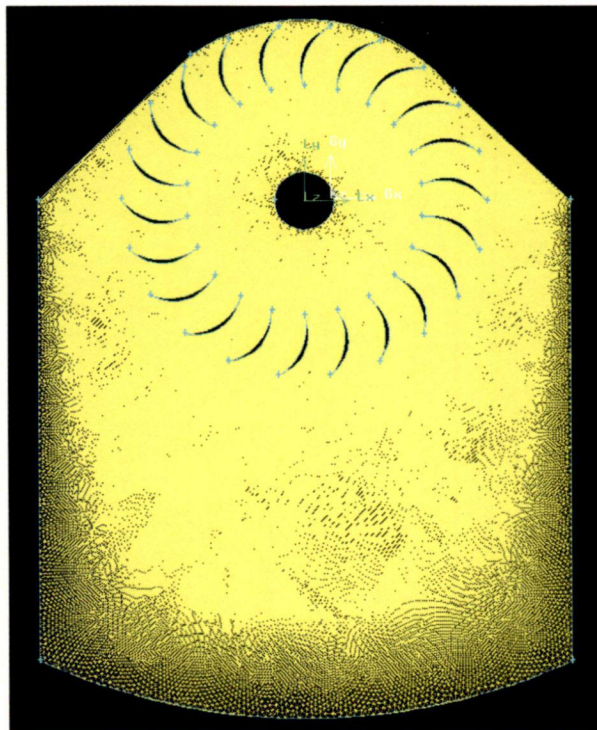


Fig 3.16 Meshed Model of full runner

3.5 FLUENT – THE SOLVER

3.5.1 General

FLUENT is a state-of-the-art computer program for modeling fluid flow and heat transfer in complex geometries. FLUENT provides complete mesh flexibility, including the ability to solve your flow problems using unstructured meshes that can be generated about complex geometries with relative ease. Supported mesh types include 2D triangular/quadrilateral, 3D tetrahedral/hexahedral/pyramid/wedge, and mixed (hybrid) meshes. FLUENT also allows you to refine or coarsen your grid based on the flow solution.

FLUENT is written in the C computer language and makes full use of the flexibility and power offered by the language. Consequently, true dynamic memory allocation, efficient data structures, and flexible solver control are all possible. In addition, FLUENT uses a client/server architecture, which allows it to run as separate simultaneous processes on client desktop workstations and powerful compute servers. This architecture allows for efficient execution, interactive control, and complete flexibility between different types of machines or operating systems.

All functions required to compute a solution and display the results are accessible in FLUENT through an interactive, menu-driven interface.

3.5.2 Program Capability

The FLUENT solver has the following modeling capabilities:

- 2D planar, 2D axisymmetric, 2D axisymmetric with swirl (rotationally symmetric), and 3D flows.
- Quadrilateral, triangular, hexahedral (brick), tetrahedral, prism (wedge), pyramid, and mixed element meshes
- Steady-state or transient flows

- Incompressible or compressible flows, including all speed regimes (low subsonic, transonic, supersonic, and hypersonic flows)
- Inviscid, laminar, and turbulent flows
- Newtonian or non-Newtonian flows
- Heat transfer, including forced, natural, and mixed convection, conjugate (solid/fluid) heat transfer, and radiation
- Chemical species mixing and reaction, including homogeneous and heterogeneous combustion models and surface deposition/reaction models
- Free surface and multiphase models for gas-liquid, gas-solid, and liquid-solid flows
- Lagrangian trajectory calculation for dispersed phase (particles/droplets/bubbles), including coupling with continuous phase; spray modeling
- Cavitations model
- Phase change model for melting/solidification applications
- Porous media with non-isotropic permeability, inertial resistance, solid heat conduction, and porous-face pressure jump conditions
- Lumped parameter models for fans, pumps, radiators, and heat exchangers
- Acoustic models for predicting flow-induced noise
- Inertial (stationary) or non-inertial (rotating or accelerating) reference frames

- Multiple reference frame (MRF) and sliding mesh options for modeling multiple moving frames.
- Mixing-plane model for modeling rotor-stator interactions, torque converters, conservation and swirl conservation and similar turbo machinery applications with options for mass.

3.5.3 Basic Steps of CFD Analysis Using FLUENT

Before we begin our CFD analysis using FLUENT, careful consideration of the following issues will contribute significantly to the success of our modeling effort.

3.5.3.1 Problem Solving Steps

Once the important features of the problem to be solved are understood, the basic procedural steps shown below are to be followed.

1. Define the modeling goals.
2. Create the model geometry and grid.
3. Set up the solver and physical models.
4. Compute and monitor the solution.
5. Examine and save the results.

3.5.3.2 Planning of CFD Analysis

- Defining the Modeling Goals.
- Creating the Model Geometry and Grid.
- Setting up the Solver and Physical Models.
- Computing and Monitoring the Solution.
- Examining and Saving the Results.
- Revising the Model.

3.5.4 FLUENT in the present study

Now that the first two steps i.e. modeling and meshing are complete, the next step is the setting up of solver and physical models. The mesh is imported in .msh format. A single precision 2D solver is used because unless the model is having features of very disparate length scale, the double precision solver is not used. As the next step grid is checked and information about grid is gathered. Once the grid is fine we move on to the solver.

The various properties of the FLUENT that are used in the present study are:

3.5.4.1 Solver

a) Segregated

There are two kinds under this category i.e. a segregated and a coupled solver. Choice of solvers depends heavily on the model being solved. The segregated solver solution is based on the pressure, while the coupled solver solution is based on density. This makes the segregated solver better at low speed flows and the coupled solver better at solving transonic / supersonic cases. A coupled solver is used for high speed incompressible flows.

b) Implicit

The explicit solver is used only with the coupled solver which is not the present case.

c) Defining Velocity Formulation

The two kinds of velocity formulation that are available in Fluent are Absolute and Relative. Absolute is chosen here because the absolute velocity formulation is preferred in applications where the flow in most of the domain is not rotating (e.g., a fan in a large room). The relative velocity formulation is appropriate when most of the fluid in the domain is rotating, as in the case of a large impeller in a mixing tank. For most applications, either formulation may be used. Since, it is an assumption that the rotational

effects are neglected; the absolute velocity formulation is used.

d) Defining Pressure Based Solver

In the latest version FLUENT 6.3 that is used for the present study there are two kinds of solvers i.e. pressure based and density based. The pressure based solver is used. This new solver can improve solution efficiency as well as convergence and robustness for many cases. With this solver scheme, the pressure and velocity equations are solved in a fully coupled manner, while the other equations are solved sequentially. It is particularly beneficial for “stiff” problems and for solving problems on unusually skewed and stretched meshes.

3.5.4.2 Defining Viscous Model

The viscous models available are In viscid, Laminar, and Turbulent. Further turbulent models available are Spallart- Almaras model, k-epsilon model, k- ω model and Reynolds Stress model. It is unfortunate fact that no single turbulence model is available as being superior over all kind of problems. The choice of turbulence model will depend upon the considerations like the physics encompassing the flow, the established practice for a specific kind of a problem, the level of accuracy required, the available computational resources and the amount of time available for the computations. The simplest "complete models" of turbulence are two-equation models in which the solution of two separate transport equations allows the turbulent velocity and length scales to be independently determined. The standard k-epsilon model in FLUENT falls within this class of turbulence model and has become the workhorse of practical engineering flow calculations in the time since it was proposed. Robustness, economy, and reasonable accuracy for a wide range of turbulent flows explain its popularity in industrial flow and heat transfer simulations. It is a semi-empirical model, and the derivation of the model equations relies on phenomenological considerations and empiricism. Thus, the model chosen for the present study is the k-epsilon model.

3.5.4.3 Defining Material

The material in the present study under the observation is water. Water is chosen under the material selection list available in the FLUENT database.

3.5.4.4 Defining Units

The units of length are changed from m (default) to mm.

3.5.4.5 Defining Operating Conditions.

The operating pressure is taken as 101325 Pascal and the gravity as -9.81 m/s^2 in the y- direction.

3.5.4.6 Defining Boundary Conditions

This is the most crucial part of any analysis. The success and failure of any analysis largely depends on the definition of boundary conditions. Various Boundary Conditions used are defined as under.

- a) Blades
 - Adjacent Cell zone is water
 - Wall motion is stationary
 - Shear Condition is No Slip
- b) Default interior is water
- c) Inlet
 - Velocity Specification Method is Magnitude Normal to the Boundary
 - Reference Frame is Absolute
 - Velocity Magnitude is 12.6 m/s
- d) Outlet
 - Gauge Pressure (Pascal) is zero. This means that the pressure at outlet is atmospheric.
- e) Shaft
 - Adjacent Cell zone is Water
 - Wall motion is Stationary
 - Shear Condition is No Slip.
- f) The material of flow is water which is selected from the FLUENT Database.

3.5.4.7 Initializing the Solution

Before starting the CFD simulation, FLUENT must be provided with an initial guess for the solution flow field. In many cases extra care has to be taken to provide an initial solution that will allow the desired final solution to be attained. The solution is initialized to Compute from Velocity Inlet.

3.5.4.8 Iterations

Solve the solution by giving the number of iterations. If the numbers of iterations given are not sufficient to converge the solution then the number of iterations can be increased.

CHAPTER 4 ANALYSIS

4.1 GENERAL

The cross flow turbines are impulse turbines and were developed in this century. In the cross flow the water is directed into the blades tangentially at about mid way on one side. The flow of water "crosses" through the empty center of the turbine and exits just below the center on the opposite side. Thus the water strikes blades on both sides of the runner. It is claimed that the entry side contributes about 75% of the power extracted from the water and that the exit side contributes the remainder. The cross flow is an impulse turbine and requires a high head to be really efficient but it will "work" on heads as low as 3'. It can be fabricated in home shops and many have been built. The designer of the home plans claim about 60% efficiency for home built turbines. There are commercial built cross flow turbines that can deliver higher efficiencies, on ideal sites.

The Cross Flow Turbine has a drum type runner on which the blades are arranged on the periphery of the supporting rings. Thus, the interior is hollow where the flow is free to flow. This empty space contains the shaft responsible for rotation of the runner due to the momentum transferred by the flow. The diameter of the shaft is the main factor which is under immense observation these days. The diameter of the shaft should be optimized between the strength and the flow. If the diameter is kept large it gives sufficient strength to the runner but the flow is obstructed before striking the second series of blades on the diametrically opposite end. The other option is that if we remove the shaft. This case makes the turbines hydraulically efficient but the mechanical strength of the runner is to be compromised with. In this case the collars have to be strengthened. The present analysis consists of analyzing various diameters and their effects on the flow. The diameters under consideration are 50.8 mm, 38.1 mm, 25.4 mm, 12.7 mm and no shaft.

4.2 ANALYSIS OF CROSS FLOW RUNNER

4.2.1 Shaft with diameter 50.8 mm

The first case is the shaft with diameter of 50.8 mm. Fig 4.1 shows the velocity contours of the flow in the turbine. The velocities with different magnitudes are shown by the different colors and are depicted in the legend shown on the left hand side of the figure. The top curve of the figure is the nozzle which is the velocity inlet of the flow. The nozzle covers 90° and the total numbers of the blades considered are 22. So the angle between the center of the shaft and any two blades is 16.36° .

As the water exits the nozzle with a speed of 12.6 m/s it travels an empty space of about 1mm which is the clearance between the nozzle and the runner. The water as it glides on the blades is flowing in constricted passage and the force of gravity makes the velocity to increase. The convex portion of the blades experiences an increase in speed more than the concave part. Thus this comparatively higher speed results in lower pressure on the convex side and relatively higher pressure on the concave side.

The thin blue lines from the entry of the blade to the exit of the blade denote the low velocity zones on the concave side of the blades. This is because the entire flow is not entering the flow at the angle of attack. Thus, the entry edge of the blade kills a certain part of the fluid which is shown by the thin blue portions. The flow when it exits the first series of blades travels through the empty space up to the shaft. As the flow reaches the shaft some part of the flow that is traveling in the middle strikes the shaft head-on. This kills the velocity of the flow which is shown by the blue portion on the above part of the shaft.

The values of velocity at the shaft are 0 m/s and a very meager 2-3 m/s on the upper blue portion. This dead flow when passes by the sides of the shaft along with the adjoining flow attains a very high speed shown by reddish yellow portion on the left and right hand side where the values of the velocities goes as high as 55-57 m/s.

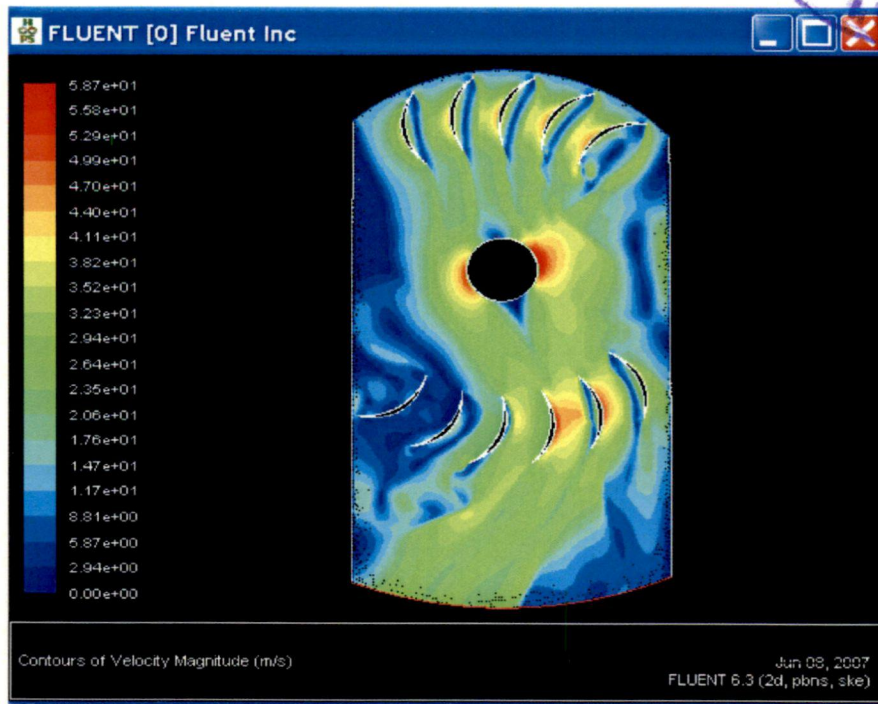


Fig 4.1 Velocity Contours of Runner with Shaft Diameter of 50.8 mm

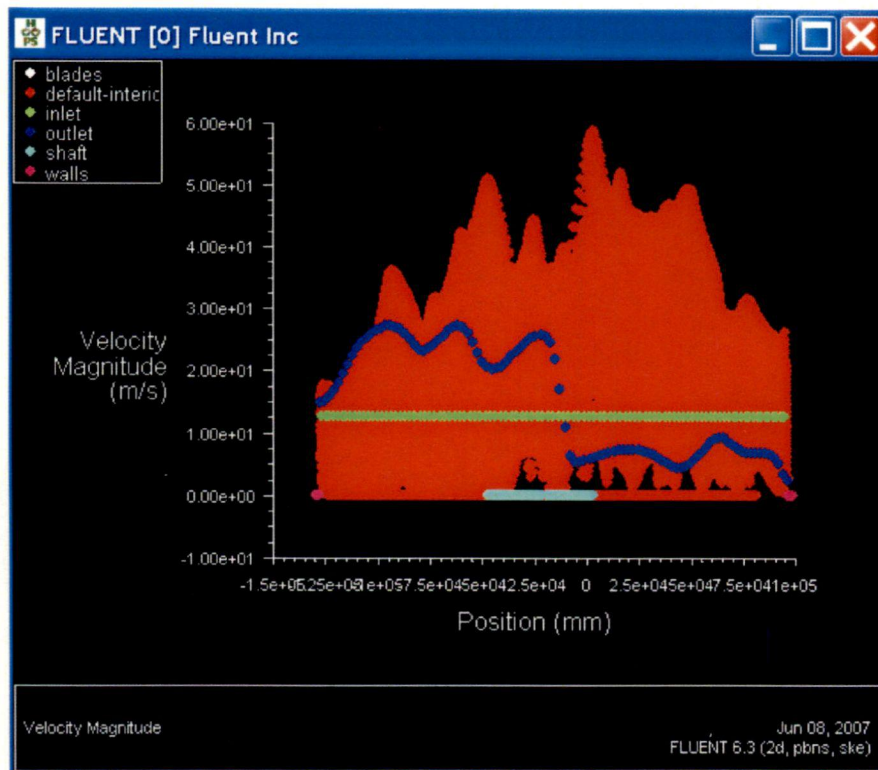


Fig 4.2 The Plot of Velocity Magnitude with respect to the position

Thus the circumference of the shaft offers a great resistance to the flow resulting in abrupt changes in the velocities. As the flow passes by the shaft, enough space is available for the flow hence it attains the speed of the flow which is around 30 m/s.

Also, on the lower portion of the shaft there is a small blue portion of low velocity zone. This is because the flow rushes past the shaft with high velocity creating a wake just below the shaft. The flow then strikes the second series of the blades and a similar phenomenon as in the above series is experienced. The convex portion experiences a high velocity zone (low pressure). Here, the point to note is that the upper series of blades have 5 blades and the lower series of blades have six blades, hence, the portion between the left two blades shows a low velocity region as it is flow deficient.

Fig 4.2 shows the plot of velocity in m/s. the X axis is the distance in mm and the Y axis shows the magnitude of velocity. The above figure shows the variation of velocity along the distance from the extreme left portion of the model to the extreme right. The green line represents the inlet velocity that is coming out of the nozzle which is constant throughout and hence is shown by the straight line. The blue curve represents the velocity at outlet. The pink dots on the eighth ends are the left and right walls. The light blue line in the middle velocity of the shaft. The red portion is the velocity of the quantum of water flowing in the model. The velocity at outlet varies from 28 m/s to 0 m/s.

Fig 4.3 shows the variation of pressure as in the pressure contours. The figure clearly shows the regions of high pressure at inlet. This indicates that the velocities at this section are low. The pressure gradually goes on decreasing along the length of the blade. The regions where the velocities are high, the pressures are low and vice versa. Again on the shaft the right hand and left hand portions which shows low pressure areas and on the same location we can see on the velocity contours that the velocities are very high. Again on the top and bottom of the shaft the pressures are very high because the velocities in this portion are extremely low.

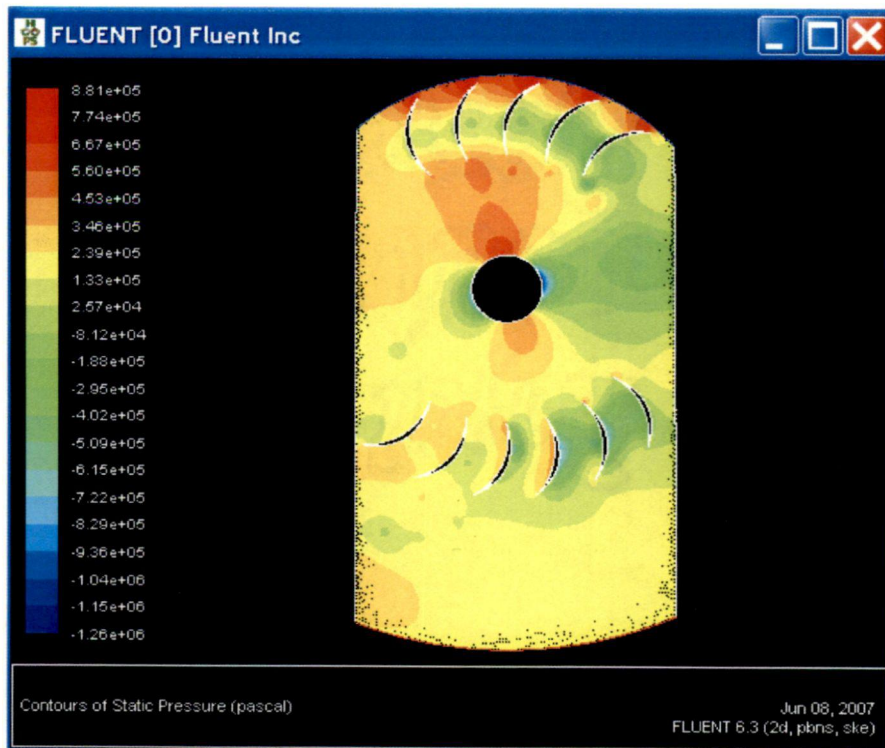


Fig 4.3 The Contours of Static Pressure for Runner with Shaft Diameter of 50.8 mm

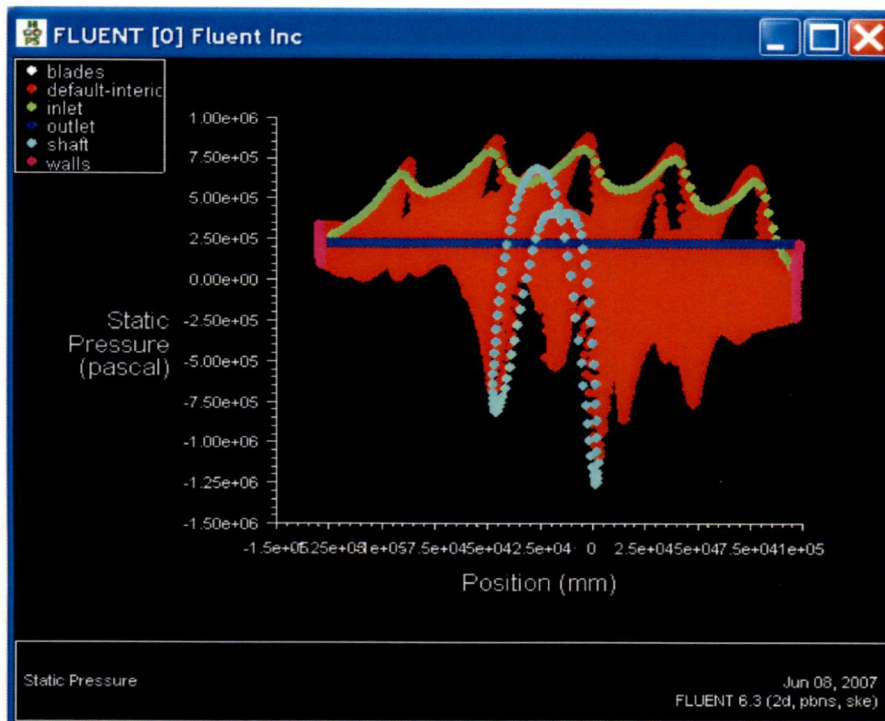


Fig 4.4 The Plot of Static Pressure with respect to the Position

The abrupt changes on the borders (i.e. the walls and the outlet) are because of the fact that the atmospheric conditions interfere with the computations in the immediate vicinity of the borders. It is precisely for this reason that the computational domain is extended at the outlet.

Fig 4.4 shows the plot of static pressure with respect to the distance. The blue line shows the pressure at outlet which is constant because of the simple fact that the outlet pressure was given to be constant at atmospheric. The pink lines at the end shows how the pressure varies on the left and right walls that are used to confine the computational domain on either end.

The pressure depicted by the green fluctuating line is the pressure at the inlet. The undulations, which are five in number shows the five blades' edges. The red region is the variation of the pressure in the quantum of water or the interior. The light blue portion is the variation of pressure on the surface of shaft. It is clearly seen that the fluctuation of pressure is maximum in the case of shaft which ranges from as low as $-1.25e+06$ to as high as $7e+05$.

4.2.2 Shaft with diameter 38.1 mm

Although the shaft with 50.8 mm diameter is mechanically most stable but hydraulically it is not good because of the obstruction it offers to the flow. So to decrease this obstruction in flow, the next case that we chose is the shaft with diameter of 38.1 mm. Fig 4.5 shows the velocity contours of the flow in the runner when the diameter is 38.1 mm. The flow in the first set of blades is almost similar as in the first case i.e. the flow enters the blades and develops a high velocity (low pressure region) on the convex side. The flow then exits the blades and strikes the shaft. The region of flow affected by the shaft is small as compared to the shaft with diameter of 50.8 mm. Fig 4.6 represents the plot between velocities at different boundaries and the position with respect to the global coordinate system. The bulk in red shows the velocity variation of the flow which varies from 57 m/s to 0 m/s. again as in the previous case the velocity is constant at inlet and is represented by the green line.

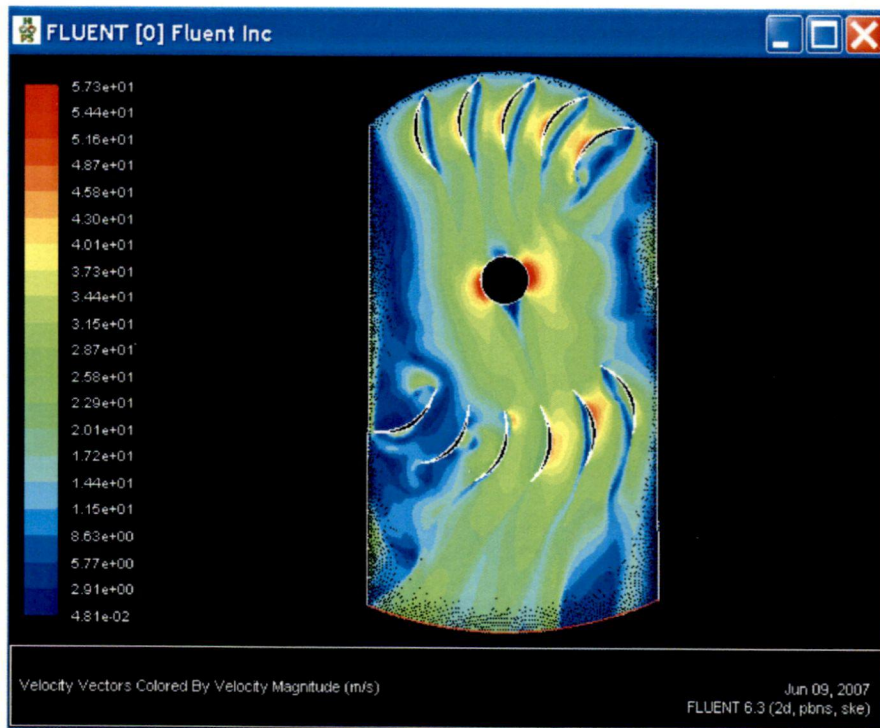


Fig 4.5 The Velocity Contours of Runner with shaft Dia of 38.1 mm

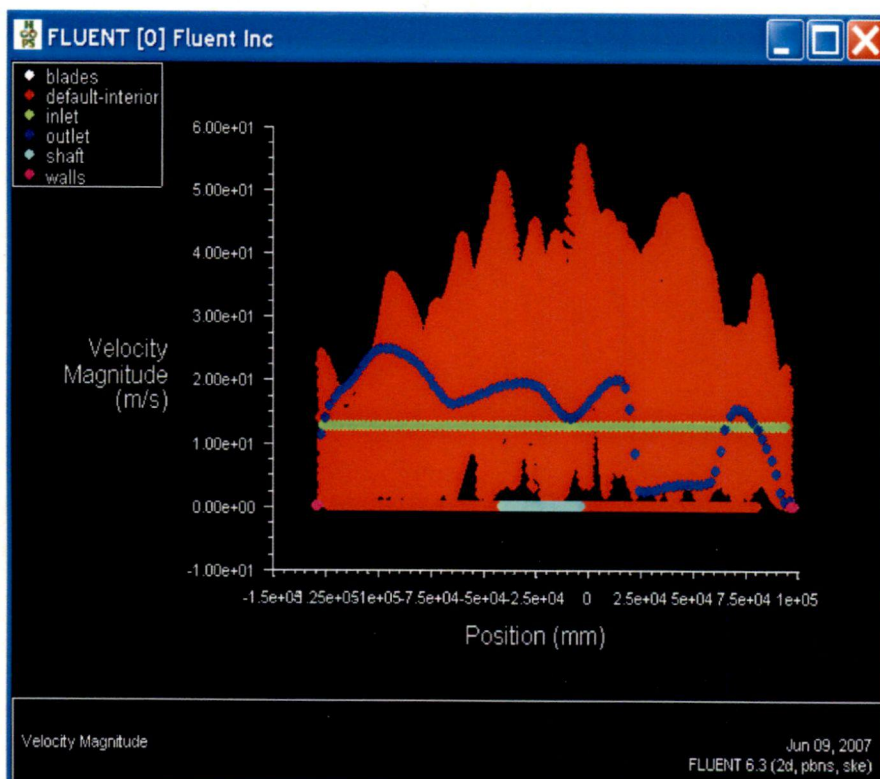


Fig 4.6 The Plot of Velocity Magnitude with respect to the Position.

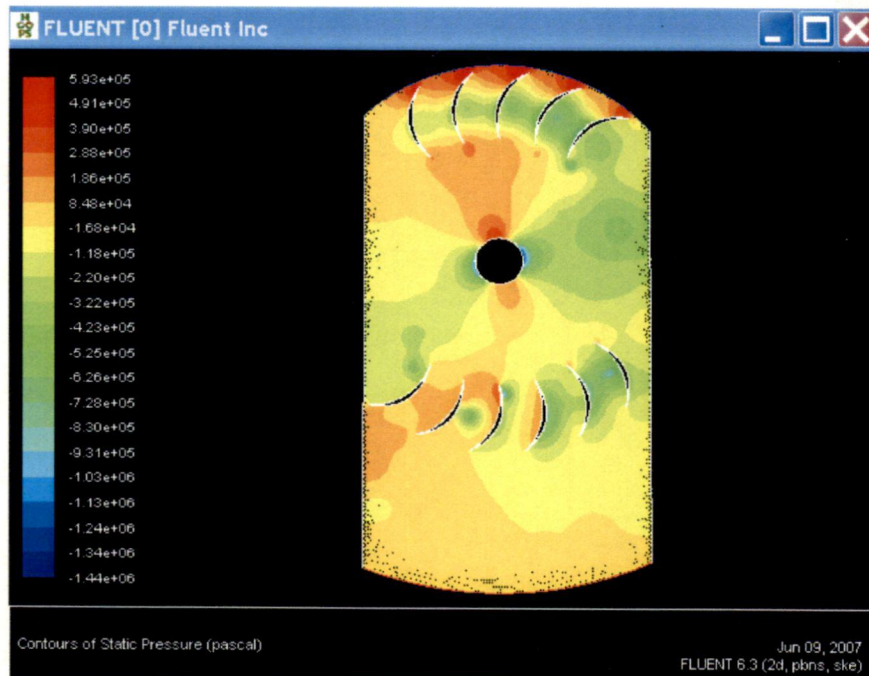


Fig 4.7 The Pressure Contours of Runner with Shaft Diameter of 38.1 mm

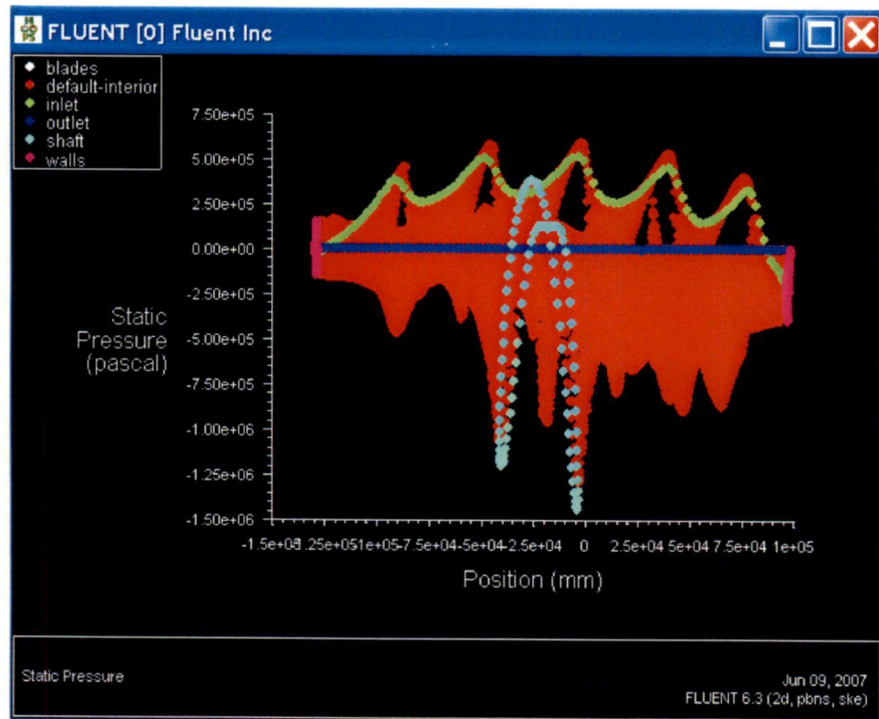


Fig 4.8 The Plot of Static Pressure with respect to the Position.

Also the blue curve represents the velocity at outlet and it varies from 0 m/s to 25 m/s. the velocity of shaft (light blue) and the sidewalls (pink) are zero. In this figure we can clearly see that the conditions of pressure are identical as in the first case at the inlet. The major difference that can be seen is between the first three blades at inlet and the shaft where the pressure is low as compares to the first case which implies that the velocities are high in this region. The fig 4.8 shows the plot of the static pressure and the position. The figure shows how the pressure varies with position at different boundaries. The pressure varies within the limit of $-1.5e+06$ to $5.6e+05$ Pascal unlike the previous case.

4.2.3 Shaft with diameter 25.4 mm

As we are gradually decreasing the diameter of the shaft, the next case under consideration is the runner with the diameter of the shaft as 25.4 mm. The Fig 4.9 shows the velocity contours for this case. As in previous two cases the velocity profiles are similar for the first set of blades. The region of variation of velocities is further narrowed down in the adjoining zone of the shaft although the values are almost the same varying from 36 m/s to 55 m/s in the left and right portions and 0 to 15 m/s on the top and bottom.

Fig 4.10 shows the plot of the velocity plot between the velocities at different boundaries and the position. Fig 4.10 shows that the velocity, in general varies from 55 m/s to 0 m/s. The different colors show the different boundaries as in previous case. The legend gives the colors which the different boundaries are represented by.

Fig 4.11 shows the contours of static pressure in the runner with the diameter of 25.4 mm. As we can see that the region of low pressure is becoming more prominent on the convex side of the second blade from the left (The round portion shown by green). This can be attributed to the reduced diameter of the shaft.

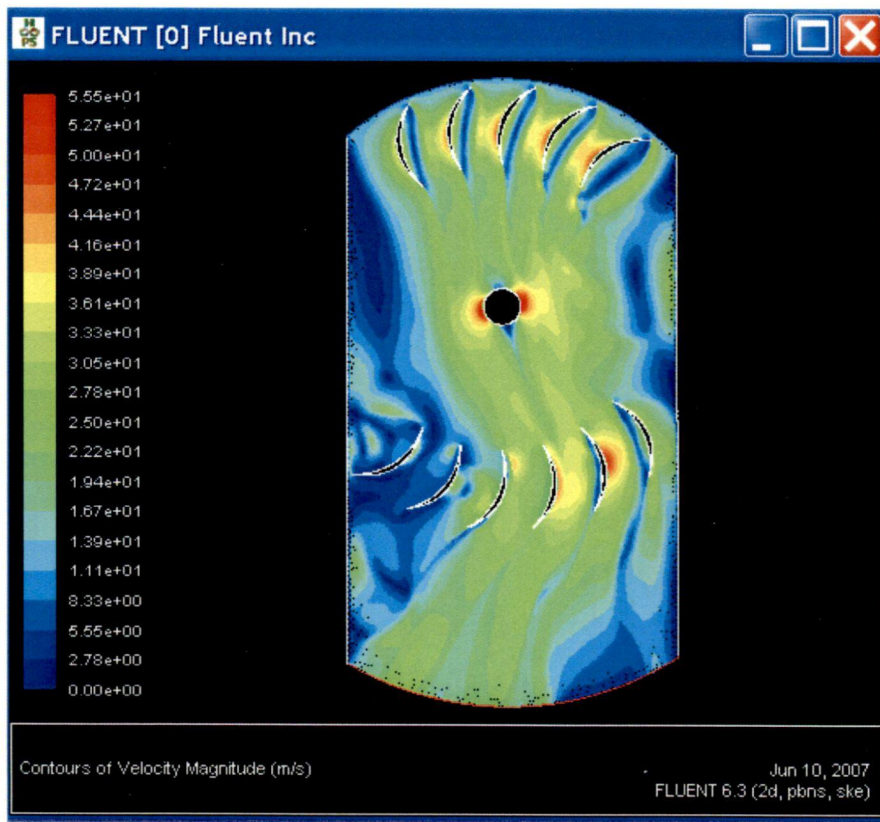


Fig 4.9 The Velocity Contours of Runner with Shaft Diameter of 25.4 mm

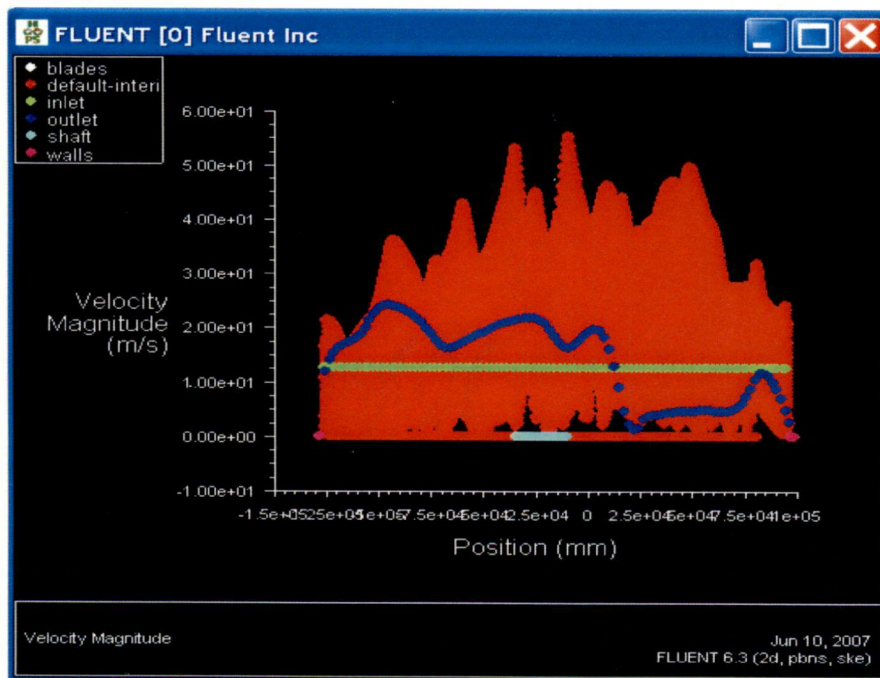


Fig 4.10 The Plot of Velocity Magnitude with respect to the Position.

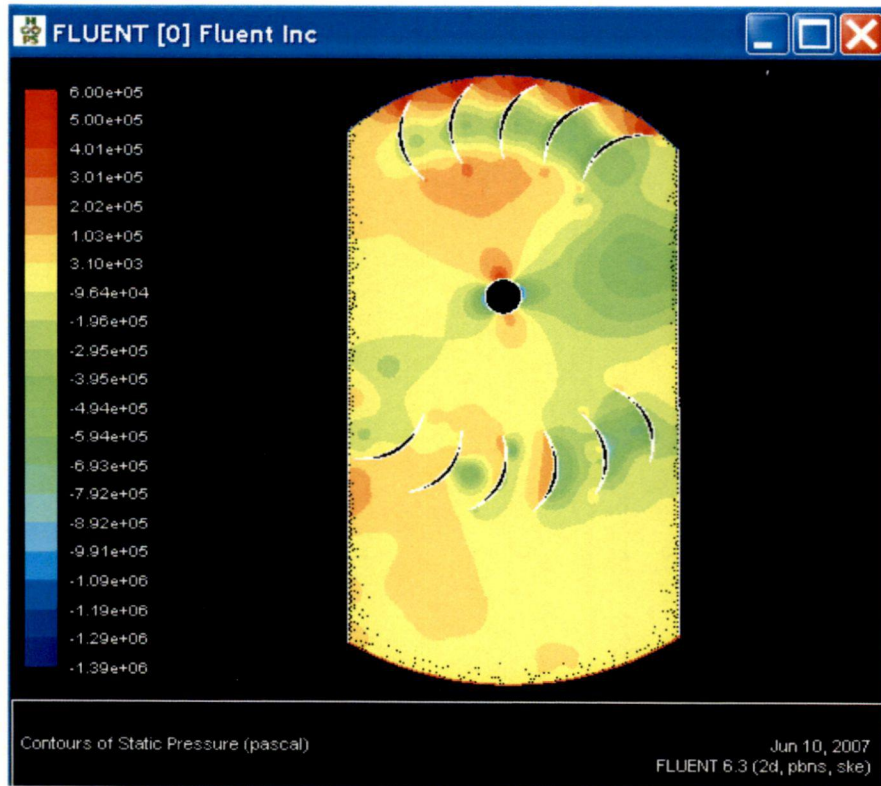


Fig 4.11. Contours of Static Pressure for Runner with Shaft Diameter of 25.4 mm.

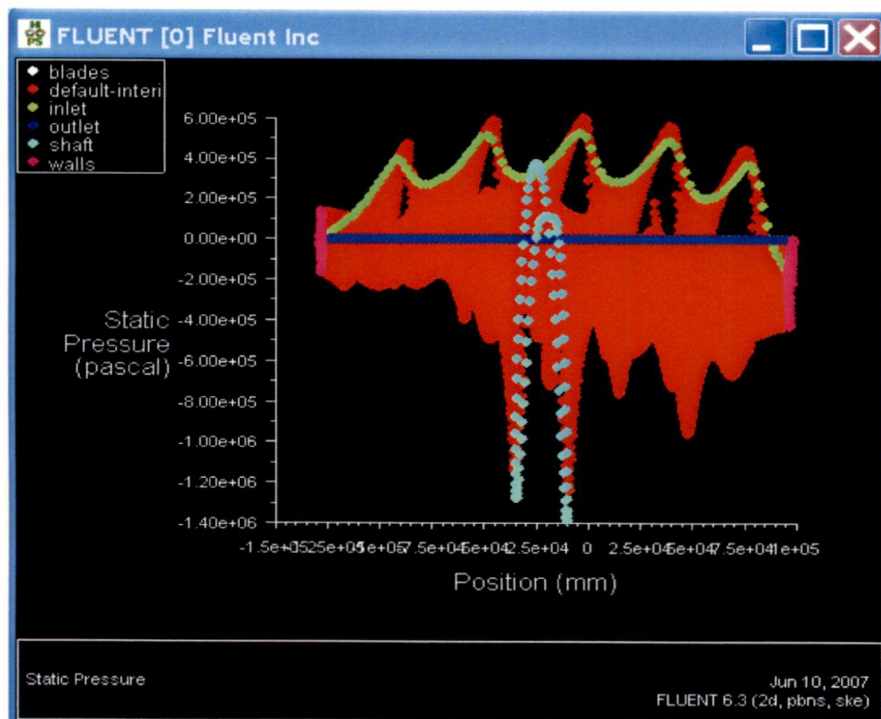


Fig 4.12 Plot of Static Pressure with respect to the Position

Fig 4.12 shows the plot of the static pressure with respect to the position. The light blue curves show the values of pressures at the shaft. The variation on the X axis on these curves is reduced because the size of the shaft is reduced. The pressure varies from $-1.4e+06$ to $6e+05$ in the entire calculation domain.

4.2.4 Shaft with a diameter of 12.7 mm.

As we decrease the diameter, the last case that that we take with shaft is the runner with shaft of diameter of 12.7 mm. This case offers minimum resistance to the flow because the diameter of the shaft is very small as compared to the diameter of the runner. The Fig 4.13 shows the velocity contours of the flow in the runner in this case. Again like the previous cases the velocity pattern is similar in the first set of blades. The variation of velocity in the adjoining region of the shaft is very small. The pattern of the variation is the same i.e. the high velocity regions at the sides and the low velocity regions at the top and bottom although the low velocity regions are practically insignificant at the top.

Also it can be seen that the flow which is low at outlet from the second set of blades as compared to the previous cases. Fig 4.14 shows the plot of velocity with respect to the position. The bulk is shown in red color again as in previous cases. The velocity is varying from 58.1 m/s to 0 m/s. again as in previous cases the velocity at inlet which is constant is shown by the green line which is constant.

The major change that can be seen from this figure is the pattern in which the velocity at outlet is varying. The variation ranges from 22 m/s to 3 m/s which is much stable from the previous cases where the variation was as high as 28 m/s to 0 m/s. Also the rise and fall of the curve of the outlet velocity is not as sharp as in the previous cases except for the last part.

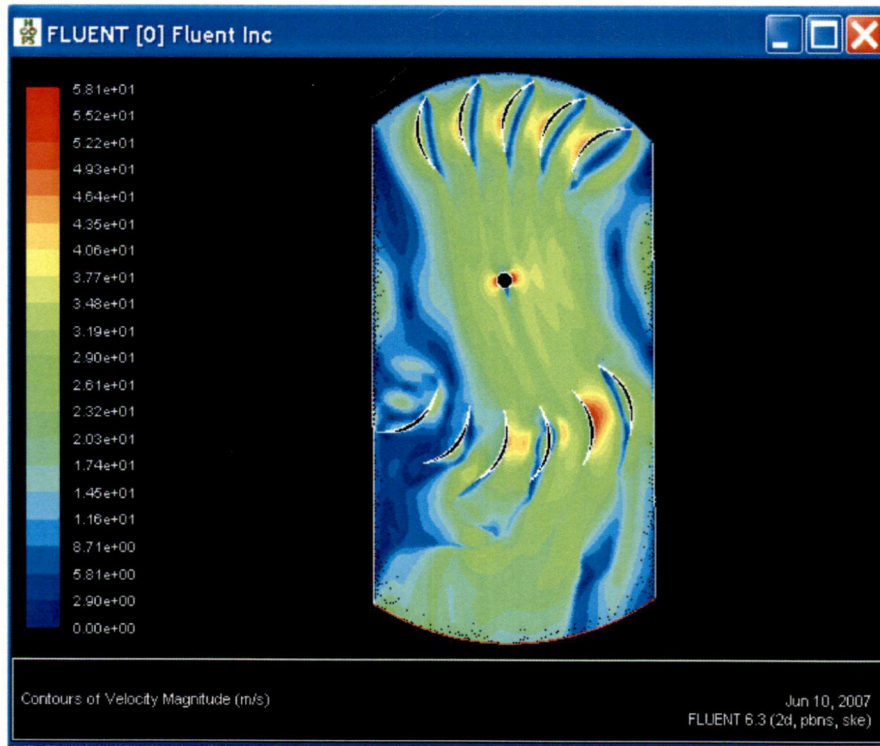


Fig 4.13 Velocity Contours for Runner with Shaft Diameter of 12.7 mm

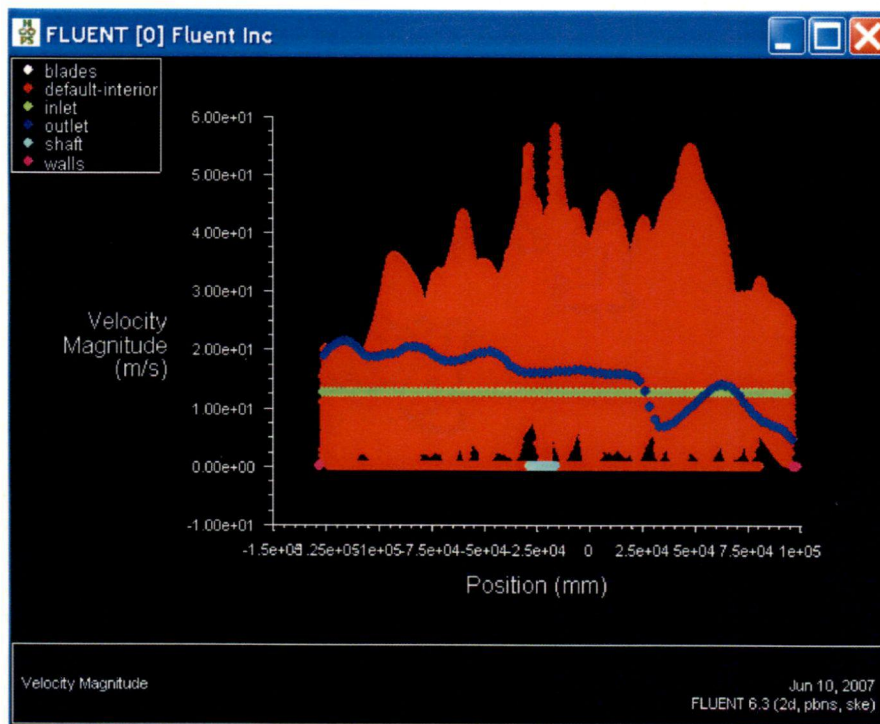


Fig 4.14 Plot of velocity with respect to the position.

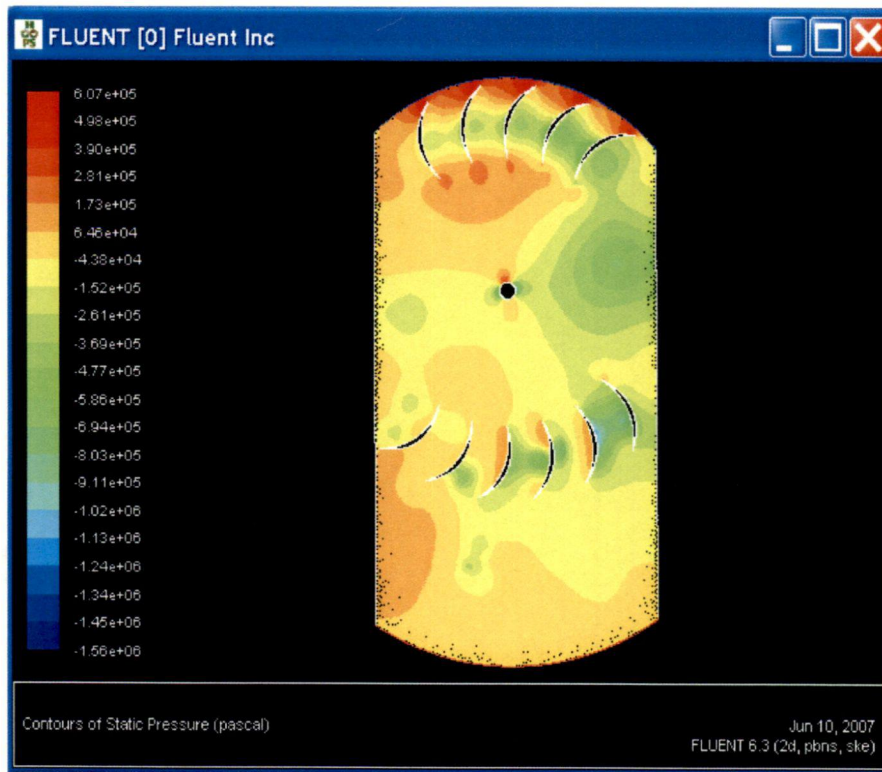


Fig 4.15 Pressure Contours for Runner with Diameter of the shaft as 12.7 mm.

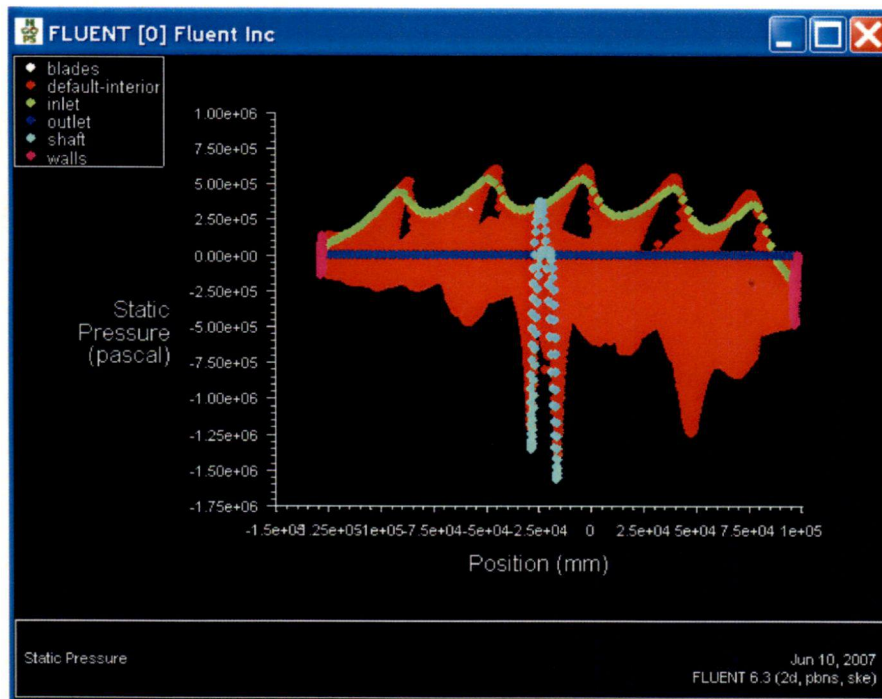


Fig 4.16 Plot of Static Pressure with Position

Fig 4.15 shows the pressure contours of the present case. The patterns of pressure for the first set of blades are the same as in previous cases. The change that can be seen is in the pressure contours between the zone that is above the shaft and below the first set of blades. The pressure between the first three blades and the shaft was quite high in the previous cases which are not as high in this case. Earlier, the entire portion was above $4.53e+05$ Pascal but here the major portion is in the region of $6.46e+04$ to $1.73e+05$ Pascal. Fig 4.16 shows the plot of pressure with respect to The Position between the curves for pressure variation at the shaft further narrows down which is in accordance with the decreased diameter of the shaft. The pressure ranges from $6.07e+05$ to $-1.06e+06$.

4.2.5 Runner with no through shaft

A case of cross flow runner having no through shaft can be analyzed. Variations in velocity and pressure over the runner having different shaft diameters have been discussed in the previous sections now the runner with no through shaft is analyzed. This will offer no resistance to the flow in the runner. The Fig 4.17 below shows the velocity contours of this case. The pattern of flow is almost similar in the first series of blades as in the previous cases. At the central portion of the runner it is seen that a high velocity region exists. Although high velocity regions were existing in the previous cases also but it was observed on either sides of the shaft and were not extended up to the second series of blades as in this case.

The maximum velocity reaching the second set of blades was in the range of 25.8 to 31.5 m/s while in this case the maximum velocity reaching the second set of blades is in the range of 31.1 to 33.5 m/s. Because of this the velocity on the convex sides of the blades second and third from right on stage II is higher.

The Fig 4.18 represents the velocity on a plot with respect to the position. The red portion shows the velocity of the quantum of water flowing inside the runner at different positions. The peaks are more consistent as compared to the previous cases.

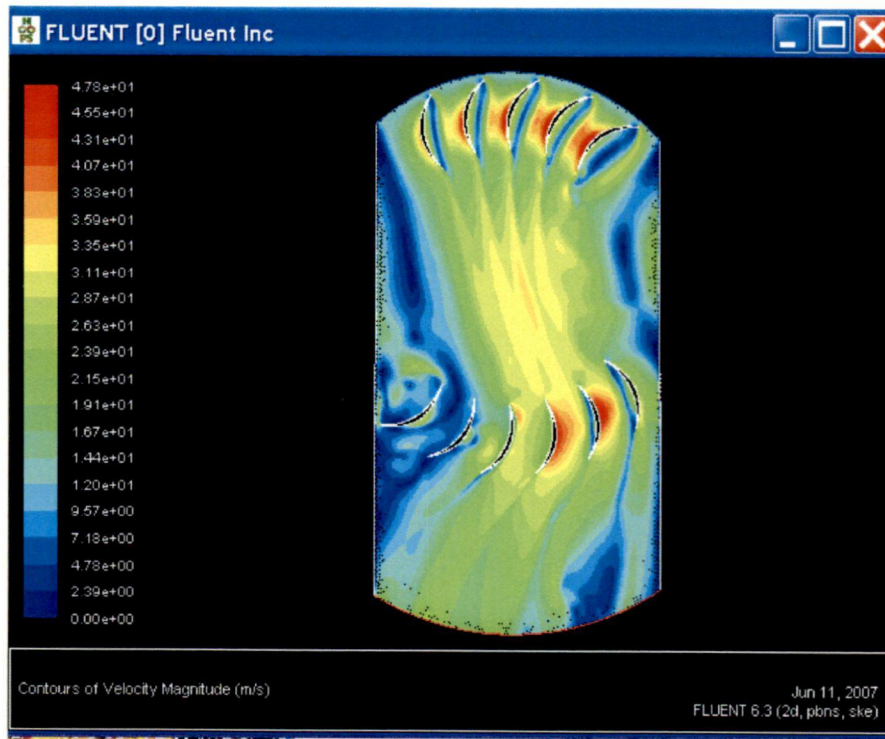


Fig 4.17 The Contours of Velocity in the Runner with no Shaft.

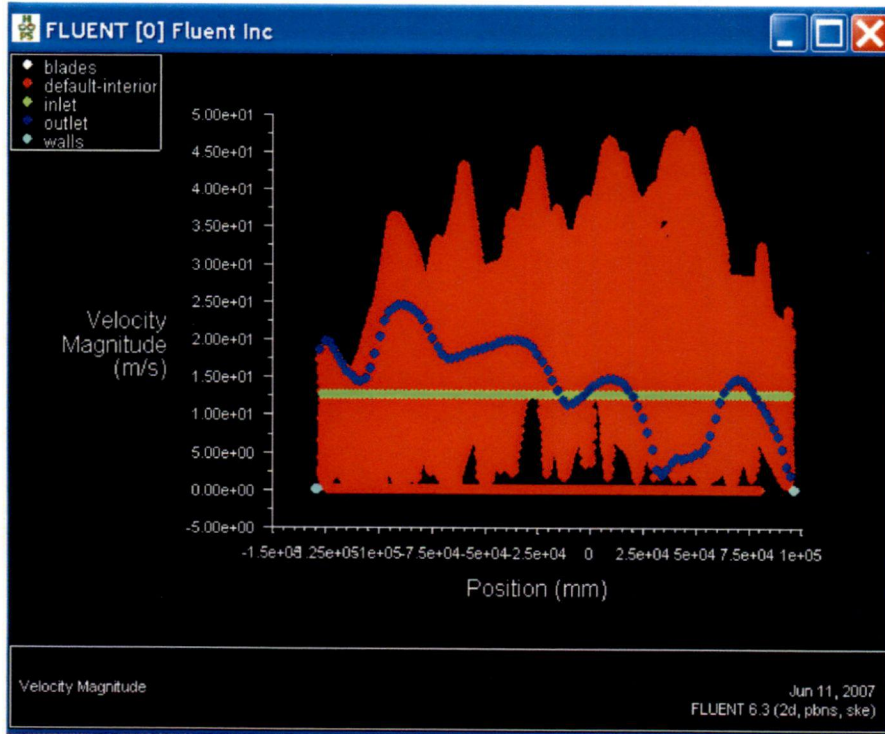


Fig 4.18 The Velocity Plot of the Runner with No Shaft

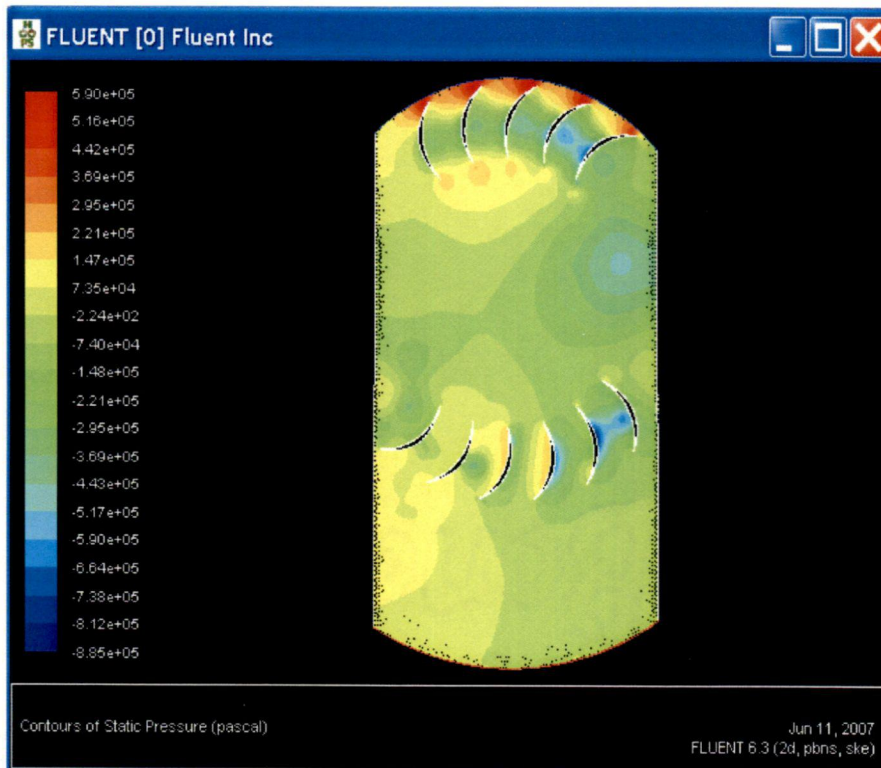


Fig 4.19 Contours of Pressure for Runner with No Shaft

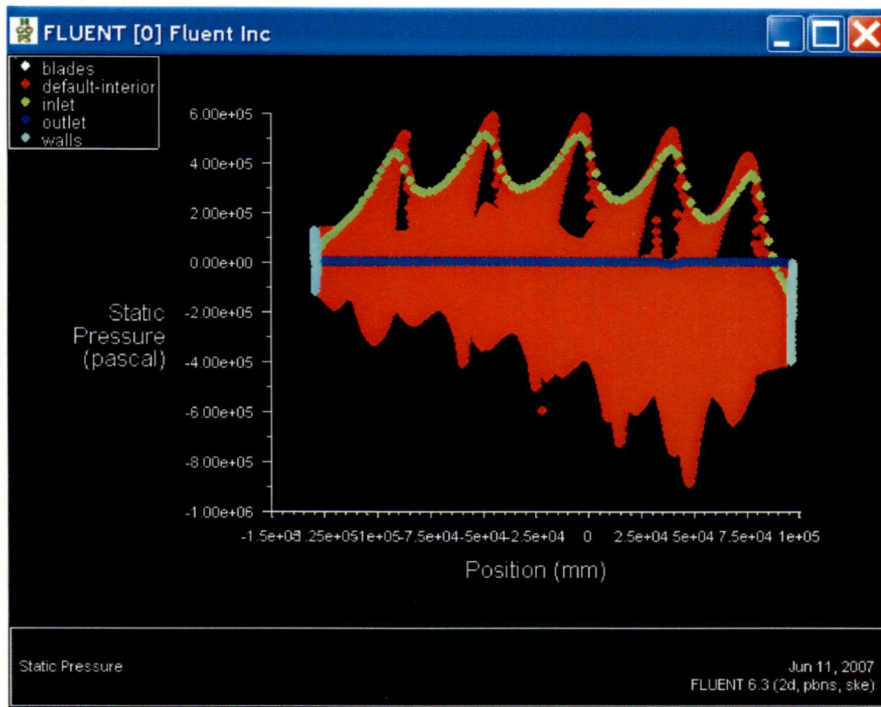


Fig 4.20 Plot of Pressure with respect to the Position

The velocity varies from 47.8 m/s to 0 m/s. The velocity at outlet shown by blue curve is again very fluctuating like first three cases and unlike shaft with diameter 12.7 mm. The Fig 4.19 shows the contours of pressure in the present case. In this figure in the central portion we can see that there is a low pressure zone as compared to the previous cases where a region of high pressure was existing between the shaft and the exit of the first set of blades. This means that the discharge is gaining velocity in this portion which can be because of gravity and no obstruction from shaft. Thus the flow is now striking the lower set of blades with high velocity and higher momentum can be transferred to the lower set of blades which is desirable. The pressure variation is from 5.90×10^5 Pascal to -8.85×10^5 .

The Fig 4.20 shows the plot of pressure with respect to the distance. In the above plot we can see that the variation of pressure is not as large in the entire calculating domain as in the previous cases. The variation is 5.90×10^5 Pascal to -8.85×10^5 Pascal while in runner with diameter of 50.8 mm it was varying as -1.25×10^6 to as high as 7×10^5 Pascal.

4.2.6 Full Runner with shaft diameter of 50.8 mm

As we know that the above iterations were done assuming that the flow is unsteady in the runner. This final simulation is done considering the entire runner and unsteady flow with a time step of 0.001 second. Fig 4.21 shows the velocity contours of the runner with shaft diameter of 50.8 mm and unsteady formulation. The velocities in the blades just below the nozzle show considerable change. The velocities in the convex parts are high and it gradually decreases till it reaches the concave part of the next blade. The velocity variation at the shaft is similar like the case in steady flow. The velocity at top and bottom are low i.e. zero at the immediate vicinity of the shaft and going up to 6.45 m/s. The velocity at the right and left sides are higher going up to 25.8 m/s near the shaft. Also, it is seen that the velocities are high at the tips of practically every blade of the runner.

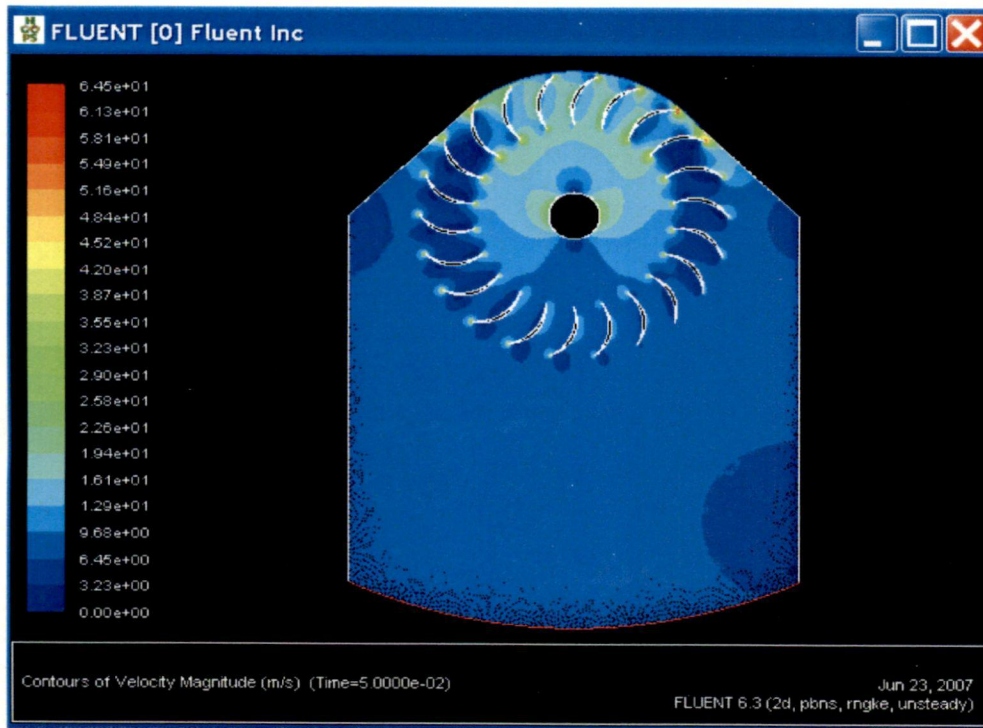


Fig 4.21 Unsteady Formulation of shaft with diameter 50.8 mm

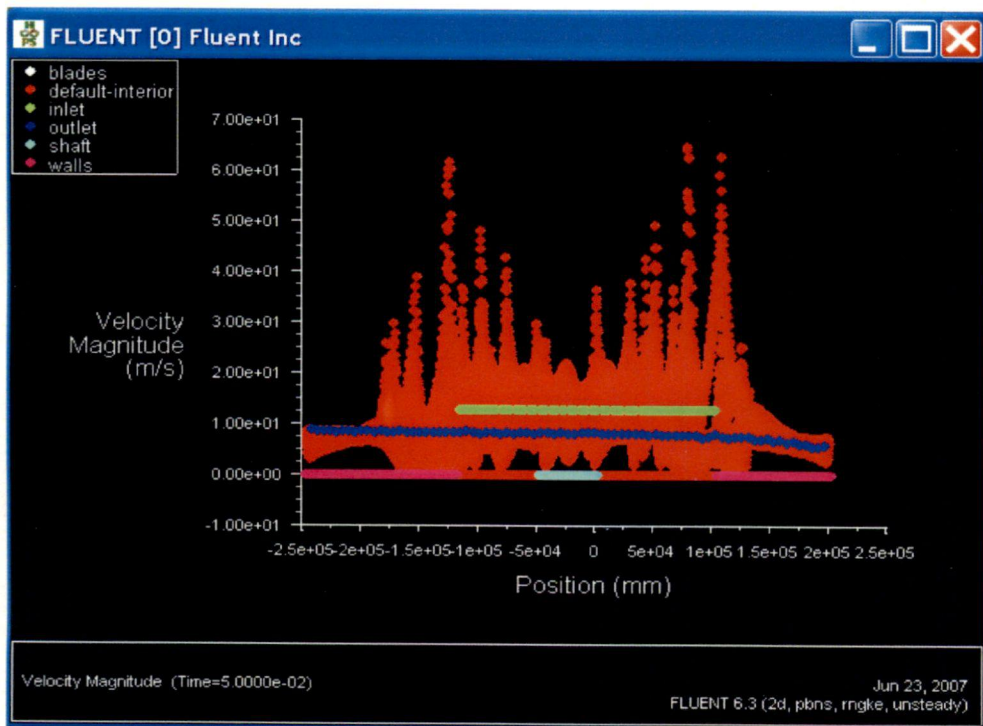


Fig 4.22 The plot of velocity with respect to the position

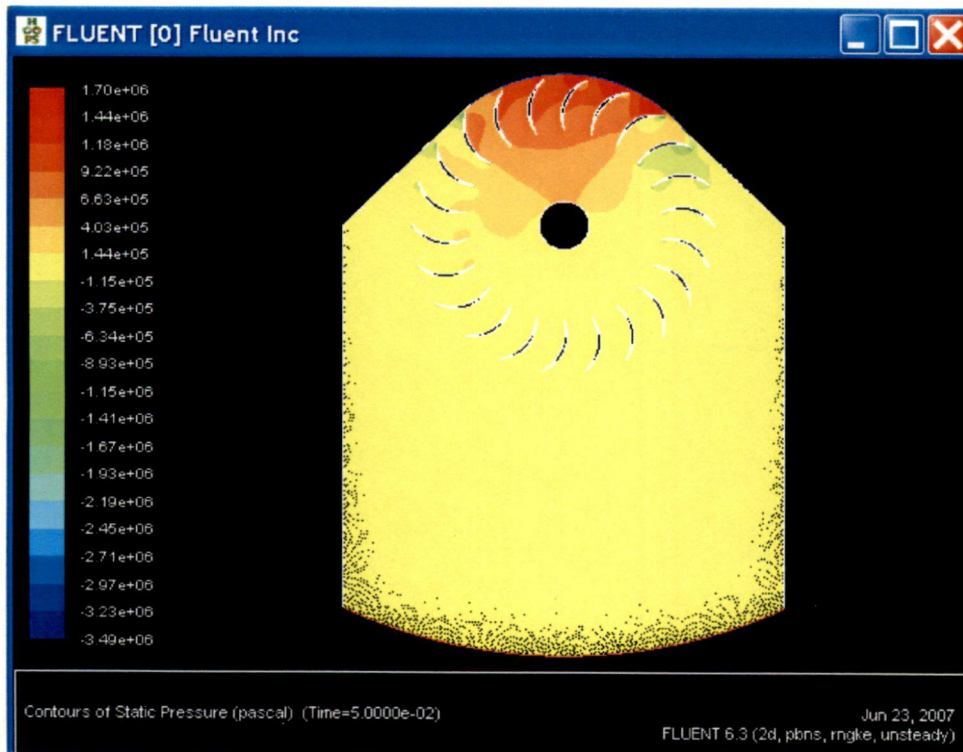


Fig 4.23 Contours of pressure for the unsteady formulation

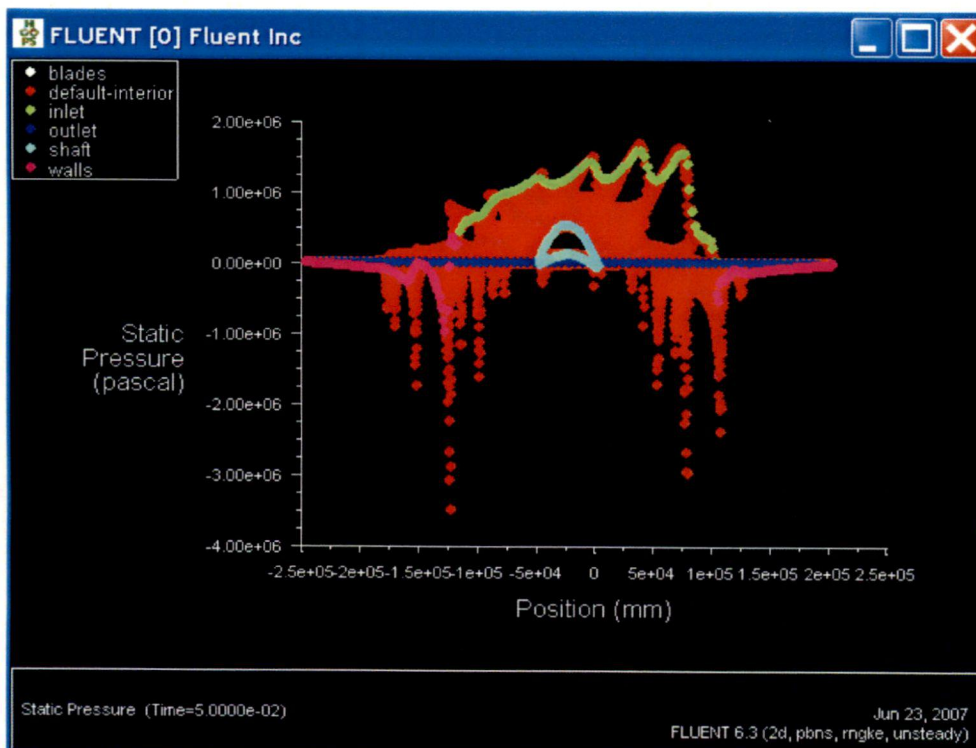


Fig 4.24 The plot of pressure with respect to the position

Fig 4.22 shows the plot of velocities with respect to the positions. The velocity at the inlet is constant by definition. The velocity at outlet is constant at around 10 m/s which is contrary with the steady state result. Also the pattern of velocity variation in the interior i.e. the velocity variation of the water is also very different. The plot shows that the major portions have low velocities but a few portions are having very high velocities shown by sharp peaks.

Fig 4.23 shows the contours of pressure in the full runner with unsteady formulation. The pressures are high at the inlet. The major portion of the computational domain has an atmospheric pressure. Also the abrupt changes in pressure are seen near the top portion of the shaft.

Fig 4.24 shows the plot of pressure with respect to the position. The plot shows the contours at inlet which show the blades. The variation of pressure at the shaft is very small as compared to the steady formulation where the pressure was ranging from -1.25×10^6 to 7×10^5 . In the present case the pressure is varying from 0 to 0.5×10^5 Pascal.

4.3 COMPARISON BETWEEN DIFFERENT MODELS

On comparing the results obtained by varying shaft diameter it is found that

- The flow pattern along the shaft is similar but the areas affected by the high and low velocity zones are different. This area is large with the shaft of diameter 5.8 mm and subsequently decreases as the diameter of shaft is decreased.
- The flow pattern around the shaft is same for steady and unsteady formulation but the magnitudes of velocity are very low in unsteady formulation as compared to the steady formulation.
- The velocities in the stage II of blades in unsteady formulation is very low and in the range of 0 to 6 m/s while in steady state these velocities were varying from 0 to 58 m/s.

CONCLUSIONS AND RECOMMENDATIONS

5.1 CONCLUSIONS

The poor manufacturing facilities for low capacity hydro turbines which are used in micro hydro power plants is a major reason for the poor performance of these machines. Keeping this in view, a flow analysis of a Cross Flow Turbine Runner is done so that the pattern of variation of velocity and pressure can be studied and presented so that these can be used to improve the performance of a Cross Flow Turbine.

Following conclusions are drawn from the present study.

1. Cross Flow Runner has a through shaft which offers resistance to the flow between the two stages.
2. The flow analysis has been done by modeling the runner of cross flow turbine, meshing it and finally analyzing it on the CFD software package FLUENT.
3. Flow pattern has been examined by varying the shaft diameter. The different values of shaft diameter taken are 50.8 mm, 38.1 mm, 25.4 mm, 12.7 mm and no through shaft.
4. The water as it glides on the blades is flowing in constricted passage and also the force of gravity makes the velocity increase a bit.
5. The convex portion of the blades experiences an increase in speed more than the convex part.
6. In the runner with shaft diameter of 50.8 mm, as the flow reaches the shaft some part of the flow that is traveling in the middle strikes the shaft head-on. The values of velocity at the shaft are 0 m/s and a very meager 2-3 m/s on the upper blue portion. Flow attains a very high speed shown by reddish yellow portion on the left and right hand side where the values of the velocities goes as high as 55-57 m/s. The flow then strikes the second series of the blades and a similar phenomenon as in the above series is experienced.

7. The abrupt changes on the borders (i.e. the walls and the outlet) are because of the fact that the atmospheric conditions interfere with the computations in the immediate vicinity of the borders.
8. In the runner with shaft diameter of 38.1 mm, the flow in the first set of blades is almost similar as in the first case. The major difference that can be seen is between the first three blades at inlet and the shaft where the pressure is low as compares to the first case.
9. In runner with shaft diameter of 25.4 mm, the region of variation of velocities is further narrowed down in the adjoining zone of the shaft although the values are almost the same varying from 36 m/s to 55 m/s in the left and right portions and 0 to 15 m/s on the top and bottom.
10. In runner with shaft diameter of 12.7 mm, the variation of velocity in the adjoining region of the shaft is very small. The pattern of the variation is the same i.e. the high velocity regions at the sides and the low velocity regions at the top and bottom of the shaft although the low velocity regions are practically insignificant at the top. Also the rise and fall of the curve of the outlet velocity is not as sharp as in the previous cases except for the last part.
11. In runner with no through shaft, as we come to the central portion of the runner we can see that a high velocity region exists. Although high velocity regions were existing in the previous cases also but they were existing on either sides of the shaft and were not extending up to the second series of blades like in this case. The peaks are more consistent as compared to the previous cases. The velocity varies from 47.8 m/s to 0 m/s as can be seen from the plot.
12. In the unsteady formulation of runner with shaft diameter of 50.8 mm, the velocities at the entire runner are in the range of 0 to 16 m/s except at the tips of the blades where the velocities are high. The velocities at the stage II of blades is very small of the order of 2-3 m/s. The pattern of the flow around the shaft is similar as in the unsteady flow with the only difference that the magnitudes of the velocities are low. Most of the variation in pressure is in the stage I of the runner and it extends up to the top of the shaft. The pressure is uniform and atmospheric elsewhere.

13. On comparing the results obtained by varying shaft diameter it is found that
- i) The flow pattern along the shaft is similar but the areas affected by the high and low velocity zones are different.
 - ii) The magnitudes of velocity are very low in unsteady formulation as compared to the steady formulation near the shaft.
 - iii) The velocities in the stage II of blades in unsteady formulation is very low as compared to steady state.

5.2 RECOMMENDATIONS FOR FUTURE WORK

The flow analysis of a cross flow runner with varying shaft diameter is presented in this study. As the future scope following recommendations are made:

- i) Similar flow analysis can be done with changed boundary conditions by considering the rotational effect of the shaft in the simulation software Fluent.
- ii) There is a scope of flow analysis by changing the design of the blades.
- iii) Flow Analysis of runner and runner as a whole can be done.
- iv) The flow analysis can be compared with the experimental results.

REFERENCES

- [1] AHEC Project Report, "Development of Standard Water Mills in Uttaranchal", October 2005, pp. 8-19.
- [2] Naidu, Dr. B.S.K (2005), "Small Hydro Highest Density, Non- Conventional, Renewable Energy Source."
- [3] CEA (1982), "Guidelines for Development of Small Hydro Electric Schemes", Government of India, New Delhi.
- [4] Baines Jeff and William Arthur, " A Test for Pico Hydro Turbines", website – www.eee.ntu.ac.uk/reasearch/microhydro/picosite
- [5] Klunne Wim, website- www.microhydropower.net/turbines.html.
- [6] website- www.usgenet.org/usa/topic/preservation/science/inventions/chpt28.htm
- [7] Joshi C.B., Sheshadri V., Singh S.N., "Parametric study on the performance of Cross Flow Turbine", Journal of Energy Engineering, Volume 121, No. 1, April, 1995.
- [8] Mockmore C.A., Merrifield F, " Tha Banki Water Turbine", Bulletin No. 25, Engineering Experiment Station, Oregon, State Coll., Corwallis, Oregon.
- [9] Balji O.E., Turbomachines John Wiley and Sons, NY, 1981
- [10] Patankar, Suhas V., (2004), " Numerical Heat Transfer And Fluid Flow", 2004.
- [11] Anderson, John D., "Computational Fluid Dynamics the basics with application".
- [12] Bhaskaran Rajesh, Caughey David, "ISTUE workshop on Dissemination of CFD Educational Interface IIHR-Hydroscience & Engineering", July 14, 2005, Iowa City, Iowa.
- [13] Balint D. et al, "Engineering Mechanics: Statics, International Student Edition," Toronto, Nelson, 2007.
- [14] Perry Ernest C., "Three Dimensional Shape Optimization of Internal Fluid Flow Systems Using Arbitrary Shape Deformation Coupled with Computational Fluid Dynamics", Department of Civil and Environmental Engineering, Brigham Young University, August 1999.
- [15] Xu Cheng, "Numerical Study of Flow and Heat Transfer in Turbo

Machinery”, The University of Wisconsin Milwaukee, December 2000.

- [16] Wen Shen Yu, “Structured and Unstructured Computations of Unsteady Turbomachinery Flows Using the Pressure Based Flows”, The Pennsylvania State University, December 2001.
- [17] Khosropanah S., “Experimental Study of Cross Flow Turbine”, Ph.D. Thesis, Colorado State University, Fort Collins, Colorado.
- [18] Desai Vengappayya Rangappayya, “A parametric Study of Cross Flow Turbine”, Ph.D Thesis, Clemson University 1996.
- [19] Bhaskaran Rajesh, Collins Lance, “Introduction to CFD basics”, January 2003.
- [20] Johnson W., Edy Y and White F, “Ultra Low Head Cross Flow Turbine- Exploratory proposal”, Rep., University of Rhode Island Kingston, Kingston, R.I.,1983.
- [21] Durgin W.W., Fay W.K., “Some Fluid Flow Characteristics of a Cross Flow type hydraulic Turbine”, Small Hydropower Machinery (1984).
- [22] Fukutomi J., Semco Y., and Nakase Y (1991), “A Numerical Method of Flow Through Cross Flow Runner”, JSME International Journal, Ser. 11, 34(1).
- [23] Nakase Y., Fukutomi J. and Watanabe T., “A Cross Flow Turbine, effect of Nozzle shape and its performance”, Small Hydro Power Fluid Machinery, Annual Winter Meeting, ASME, NY, 1982.
- [24] Marquis J. A., “Design of Evaluation of Micro Hydro Turbines (5 hp)”, Proc, Water Power '83: American International Conference on small scale Hydropower, Tennessee Valley Authority (TVA) and U.S. Corps of Engineers, Washington DC, 177-186,1983.
- [25] FLUENT Documentation, 2005
- [26] Website- www.fluentusers.com
- [27] Website- www.cfdonline.com